AD-A159 128 REVIEW OF METHODS FOR GENERATING SYNTHETIC SEISMOGRAMS (U) COLD REGIONS RESEARCH AND ENGINEERING LAB HANOVER NH L PECK JUN 85 CRREL-85-10 1/1

UNCLASSIFIED F/G 8/11 NL

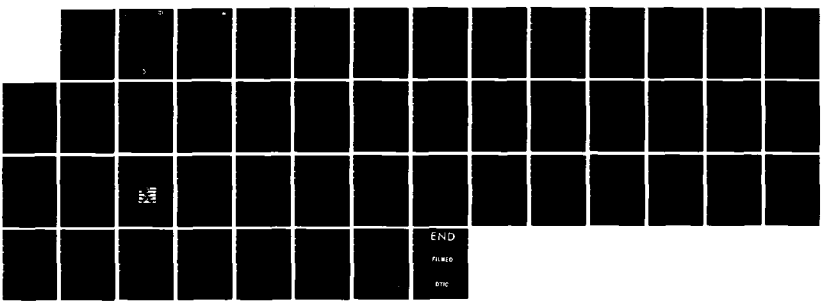

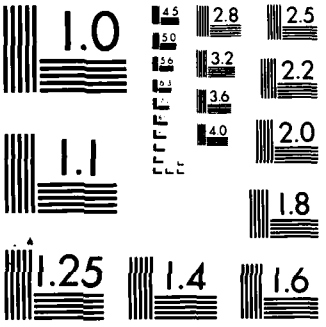

MICROCOPY RESOLUTION TEST CHART
NATIONAL BUREAU OF STANDARDS 1963 A

CRREL
REPORT 85-10

US Army Corps of Engineers
Cold Regions Research & Engineering Laboratory

Review of methods for generating synthetic seismograms

AD-A159 128

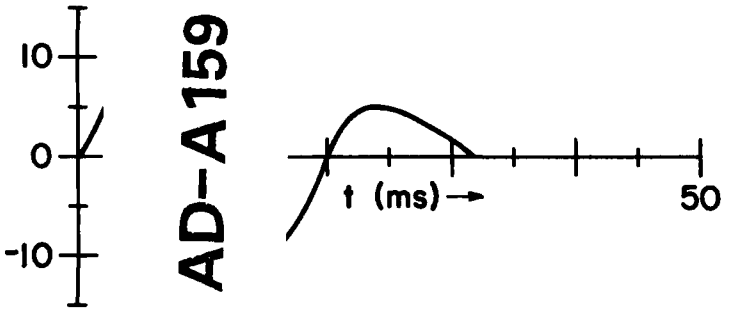

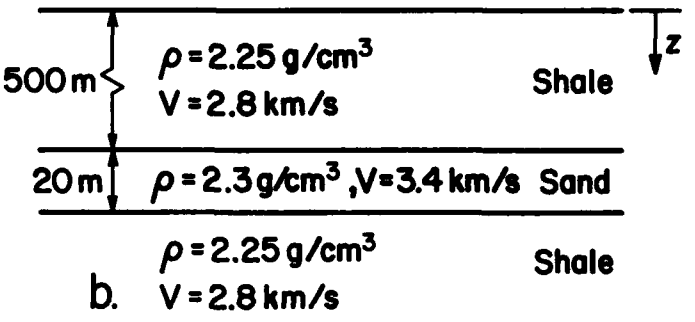

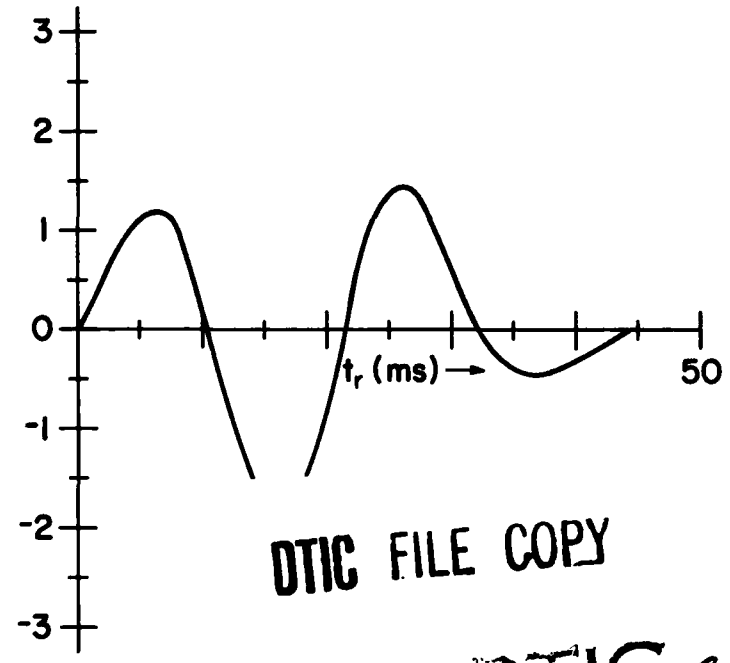

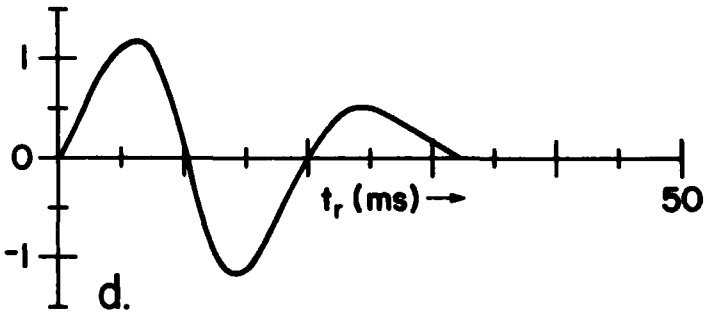

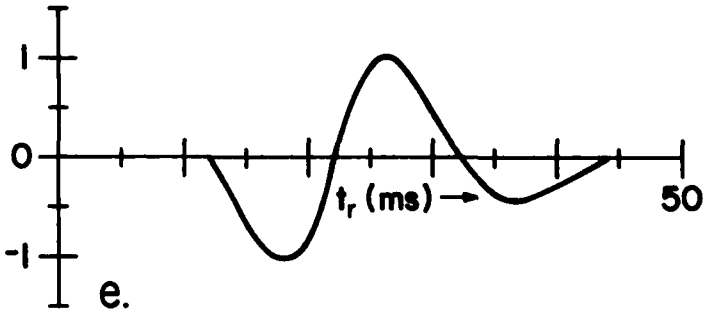

DTIC FILE COPY

DTIC
ELECTE
SEP 1 2 1985
A

85 9 10 011

CRREL Report 85-10

June 1985

Review of methods for generating synthetic seismograms

Lindamae Peck

DTIC COPY INSPECTED

By
Distribution
Availability
Dist Special
A-1

Prepared for
OFFICE OF THE CHIEF OF ENGINEERS

Approved for public release; distribution is unlimited.

REPORT DOCUMENTATION PAGE

READ INSTRUCTIONS BEFORE COMPLETING FORM

1. REPORT NUMBER: CRREL Report 85-10
2. GOVT ACCESSION NO.: AD-A159 128
3. RECIPIENT'S CATALOG NUMBER:

4. TITLE (and Subtitle): REVIEW OF METHODS FOR GENERATING SYNTHETIC SEISMOGRAMS
5. TYPE OF REPORT & PERIOD COVERED:
6. PERFORMING ORG. REPORT NUMBER:

7. AUTHOR(s): Lindamae Peck
8. CONTRACT OR GRANT NUMBER(s):

9. PERFORMING ORGANIZATION NAME AND ADDRESS: U.S. Army Cold Regions Research and Engineering Laboratory, Hanover, New Hampshire 03755-1290
10. PROGRAM ELEMENT, PROJECT, TASK AREA & WORK UNIT NUMBERS: DA Project 4A161102AT24, Task B, Work Unit 005

11. CONTROLLING OFFICE NAME AND ADDRESS: Office of the Chief of Engineers, Washington, D.C. 20314
12. REPORT DATE: June 1985
13. NUMBER OF PAGES: 48

14. MONITORING AGENCY NAME & ADDRESS (if different from Controlling Office):
15. SECURITY CLASS. (of this report): Unclassified
15a. DECLASSIFICATION/DOWNGRADING SCHEDULE:

16. DISTRIBUTION STATEMENT (of this Report)

Approved for public release; distribution is unlimited.

17. DISTRIBUTION STATEMENT (of the abstract entered in Block 20, if different from Report)

18. SUPPLEMENTARY NOTES

19. KEY WORDS (Continue on reverse side if necessary and identify by block number)

Geophysics
Ground motion
Mathematical analysis
Seismic signatures
Seismology
Synthetic seismograms

20. ABSTRACT (Continue on reverse side if necessary and identify by block number)

Various methods of generating synthetic seismograms are reviewed and examples of recent applications of the methods are cited. Body waves, surface waves, and normal modes are considered. The analytical methods reviewed include geometric ray theory, generalized ray theory (Cagniard-de Hoop method), asymptotic ray theory, reflectivity method, full wave theory, and hybrid methods combining ray theory and mode theory. Two numerical methods, those of finite differences and finite elements, and a hybrid method combining finite differences with asymptotic ray theory are described. Limitations on the application or validity of the various methods are stated.

PREFACE

This report was prepared by Dr. Lindamae Peck, Geophysicist, of the Geophysical Sciences Branch, Research Division, U.S. Army Cold Regions Research and Engineering Laboratory. Funding for this research was provided by DA Project 4A161102AT24, *Research in Snow, Ice, and Frozen Ground,* Task B, *Cold Regions Environmental Interactions,* Work Unit 005, *Computational Methods for Seismic Wave Propagation in Cold Regions.*

The author thanks Donald G. Albert and Dr. Jerome B. Johnson for technically reviewing the manuscript of this report.

CONTENTS

ILLUSTRATIONS

Figure

TABLES

Table

NOMENCLATURE

a, b	coefficients
c	velocity; phase velocity
f	dimensionless imaginary number in wave potential for refracted wave when angle of refraction is complex; function; frequency
i	$\sqrt{-1}$
k	wave number = $\frac{2\pi}{\lambda}$
$m(t)$	source term in full wave theory
n	index of refraction; mode number
p	ray parameter = $\sin\theta/c$; time level in finite difference scheme
$q(p, \epsilon)$	$[\frac{\epsilon^2}{r^2\alpha^2(\epsilon)} - p^2]$
r	range, = $\sqrt{x^2+y^2}$ or = $\sqrt{x^2+y^2+z^2}$; radial distance from the center of the earth
r_e	radius of the earth
s	imaginary parameter analogous to wave frequency
t	time
u, w	displacement
$u^P_{m,n}$	notation for displacement at a point $(m\Delta x, n\Delta z)$ at a time $p\Delta t$ in finite difference scheme
x, y, z	Cartesian spatial coordinates
$\Delta x, \Delta z, \Delta t$	spacing between points in a space-time grid in finite difference scheme
A, B	amplitudes
C	velocity; amplitude
$C(p)$	product of all reflection and transmission coefficients for a ray
C_r	velocity of Rayleigh wave at the surface of a half-space
$[C]$	damping matrix in finite element scheme
E	amount of energy per unit time per unit solid angle
$F(w)$	source time function
G	Green's function
H	Heaviside function; width of a waveguide or thickness of a layer
H_0	Hankel function
I	intensity of wave (amount of energy per second crossing a unit area)
K_0	modified Bessel function
$[K], [A], [G]$	stiffness matrix or related matrix in finite-element scheme
M	amplitude
$[M]$	inertia matrix in finite-element scheme
P	pressure field
$\{P\}$	time-independent, complex force amplitude
$\{Q\}$	column vector representing external forces applied to nodal points of a finite element grid
R	$\sqrt{r^2+z^2}$; reflection coefficient
R_{pp}	reflectivity (composite reflection coefficient)
S	coordinate distance measured along a ray; amplitude
T	period of wave; phase function; transmission losses; travel time
U	group velocity; displacement
V	velocity
W	wave front
X, Z	Cartesian spatial coordinates

α	compressional wave velocity
β	shear wave velocity
λ	Lamé constant; wavelength
μ	Lamé constant (rigidity)
σ	$\lambda+2\mu$
ρ	density
ω	angular frequency $= \frac{2\pi}{T} = Vk$
Δ	angular separation between source and receiver measured from center of earth
τ	travel time of a ray; phase shift
$\tau(p)$	$T(p)-pX(p)$
θ	angle of incidence or angle of emergence
$\theta(p)$	$pr\Delta+\tau(p)$
δ	imaginary part of complex angle of refraction; displacement
$\{\delta\}$	column vector representing displacement field of nodal points in finite-element grid
γ	parameter analogous to radial wave number; angle of incidence
υ_1	$\sqrt{k_{\alpha_1}^2 - k_{\alpha_m}^2 \sin^2 \gamma}$
$\Lambda(t)$	time series in full wave theory
η_α	$[(1/\alpha^2) - \rho^2]^{1/2}$
ϵ	arbitrary radius
ϕ, Φ	wave potential
ψ	wave potential
Γ	$[\lambda(x)+2\mu(x)]\ (\partial u/\partial x)$, *P*-waves or $\mu(x)\ (\partial u/\partial x)$, *S*-waves
π	3.14159...
*	convolution
Im	imaginary part of a complex number or function
Re	real part of a complex number or function

REVIEW OF METHODS FOR GENERATING SYNTHETIC SEISMOGRAMS

Lindamae Peck

SECTION 1. INTRODUCTION

A seismogram is a time record of ground motion. Displacements from the rest position of the recording instrument correlate with the arrival of various seismic waves at the location of the instrument, although identification of the waves and determination of precise arrival times may be difficult because of the presence of noise on the seismogram. The characteristics of a seismogram (wave arrivals, time between arrivals, amplitude and direction of displacements) are determined by the nature of the source, the structure of the earth along the wave path, and the characteristics of the receiver (recording instrument). The equivalent information is required to create a synthetic seismogram: a mathematical representation of the source, a model of the geology between source and receiver, and a surface position designated as the location of the receiver, which is modeled mathematically in terms of its response characteristics. The model of subsurface geology is usually simplified to represent gross structural features and ignore details of the geology (if known) in the vicinity of the source and receiver. The characteristics of a synthetic seismogram are most sensitive to features (velocity and density profiles, layers, irregular structure) of the geological model employed.

The usefulness of a synthetic seismogram lies in how closely it duplicates actual seismograms. The degree of correlation between the two is a measure of the accuracy of the geological model used in computing the synthetic seismogram. When a structure on the scale of the Earth itself is modeled, an Earth model that results in a close match between synthetic and actual seismograms is unlikely to be unique. Usually, however, a selection among the models can be made based upon independent criteria such as consistency with petrological or thermodynamic models of the Earth's interior. When structure on the scale of a few kilometers or less is modeled, the problem of the uniqueness of the model is less and the model is often sufficiently well constrained on the basis of surface geology or seismic surveys.

Synthetic seismograms are constructed for several purposes. They are useful in investigations of the geology of an area. The correlation between recorded and synthetic seismograms aids in the construction and refinement of a geologic model of the area. Based on a preliminary model so obtained, the deployment of seismic surveys to resolve the subsurface structure can be done efficiently and relatively economically. In this way, a synthetic seismogram is useful as a reconnaissance tool and provides information necessary for engineering site studies. Other applications

PREVIOUS PAGE IS BLANK

of synthetic seismograms require a previous knowledge of the geology. When a sufficiently accurate geologic model is known, synthetic seismograms can be used to predict the effects of explosions or earthquakes (the amplitude of the ground motion at a site due to a source of given magnitude) or to derive a theoretical model of vehicle-generated or artillery-generated ground motion for use in detection and classifier design.

The validity of a synthetic seismogram is dependent upon the accuracy of the geologic model employed, the applicability of the assumptions inherent in the derivation of the wave equation, and the approximations incorporated in the solution to the wave equation.

The wave equation is derived from a statement of the balance of forces acting on a unit volume of unbounded medium (e.g. Grant and West 1965, Officer 1974, Aki and Richards 1980). Several assumptions generally are made that result in a wave equation of the form

$$\frac{\partial^2}{\partial t^2} = c^2 \left(\frac{\partial^2}{\partial x^2} + \frac{\partial^2}{\partial y^2} + \frac{\partial^2}{\partial z^2}\right)$$

where t is time, c is velocity, and x,y and z are spatial (Cartesian) coordinates. One assumption in deriving this equation is that external forces such as gravity acting on the medium may be neglected. A second is that the medium is linearly elastic; this determines the form of the stress-strain relation that is substituted in the balance of force equation. A third is that the medium is homogeneous and isotropic and therefore the elastic parameters (e.g. the Lamé constants) of the medium are not functions of the spatial coordinates.

A synthetic seismogram is generated by solving the wave equation subject to the constraint that the boundary conditions of the problem are satisfied. The boundary conditions pertain to the components of stress and displacement at the free surface of the medium, at any interfaces within the medium, and at infinite depth in the medium. Various analytic and numerical methods are available for use in solving the wave equation; a distinction among them is that, in general, analytic methods yield an approximate solution to the wave equation while numerical methods yield an exact solution to an approximation of the wave equation. The selection of a particular method is based upon the wave types that are to be represented in the seismogram and on the degree of structural complexity that the method of generating the seismograms is capable of handling.

This report presents a description and evaluation of commonly used methods of generating synthetic seismograms. Its intent is to indicate the strengths and weaknesses of the methods and to provide examples of recent applications of them. The cited literature serves as an initial reference for individuals to use in pursuing an approach to a particular problem. A concern of this report is to identify methods capable of generating synthetic seismograms for physical situations such as thin beds or near-surface velocity inversions that are typical of winter seismological conditions. The mathematical representation of source characteristics and receiver response is not considered here; the cited references and general texts such as that of Aki and Richards (1980) show how such factors are incorporated in the process of generating synthetic seismograms.

SECTION 2. WAVE PROPAGATION IN THE EARTH

The types of seismic waves are distinguished by particle motion and velocity of propagation. The compressional wave (or synonymously the irrotational wave, longitudinal wave, dilatational wave or *P*-wave) propagates at a velocity of $\alpha = \sqrt{(\lambda+2\mu)/\rho}$ through an isotropic, homogeneous medium that is alternately condensed and rarefied; the particle motion is parallel to the direction of wave propagation. Here, λ and μ are the Lamé constants and ρ is the density of the medium. The shear wave (or synonymously the rotational wave, transverse wave or *S*-wave) propagates at

a velocity $\beta = \sqrt{\mu/\rho}$; distortion of the medium is in the plane perpendicular to the direction of propagation and is designated as *SH* (horizontal) or *SV* (vertical) depending on its orientation. The *P*- and *S*-waves are body waves.

Rayleigh waves are coupled *P-SV* waves with motion that at the surface defines an ellipse perpendicular to the surface and that exponentially decays in amplitude with depth; the waves are dispersive (propagation velocity depends on frequency) in a layered medium and nondispersive (with a velocity C_r equal to 0.9194β when Poisson's ratio is ¼) when propagating at the surface of a half-space of shear velocity β. Love waves are *SH* waves that propagate sinusoidally within a layer, decay exponentially with depth outside the layer, and exhibit dispersion; the velocity of the waves approaches the shear velocity of the surface layer in the limit of high frequencies and approaches the (higher) shear velocity of the underlying half-space in the limit of low frequencies. Rayleigh waves and Love waves are called surface waves. They are generated along with body waves (unless the source is located at a depth such that surface waves are not excited) and propagate horizontally at the surface with an attenuation due to geometrical spreading that is proportional to $1/(\text{range})^{1/2}$. Since body waves are attenuated as $1/r$ and head waves (see below) as $1/r^2$, the major portion of the wave energy reaching points distant from the source is carried in surface waves. Surface waves are viewed as noise to be eliminated when vertically or near vertically incident (reflected) waves are of interest, as is typically the case in exploration seismology, or as useful counterparts to body waves when analyzed to extract information on source parameters and earth structure between source and receiver. Because of the conditions under which they exist and the manner in which they propagate, surface waves are exceptionally well suited for use in the delineation of near-surface layered structure.

Diffracted waves are present when plane waves are incident on a feature that has a radius of curvature less than or equal to the wavelength of the incident waves. A discontinuous boundary (such as a geologic bed displaced by a fault) or a nonplanar boundary commonly causes diffracted waves to be present in the wavefield. At distances from the diffracting source that are large relative to wavelength, Huygens' construction (e.g. Halliday and Resnick 1974) is used to determine the diffracted wave energy at a particular location.

A point source in a homogeneous, isotropic medium generates *P*-waves (and *S*-waves if the medium is nonfluid) that radiate in spherical fronts; i.e. the waves propagate in all directions from the source and points of the medium that are in the same phase of motion are located on surfaces (wave fronts) that define spheres. As a wave propagates away from the source, the radius of curvature of its wave fronts increases and the wave fronts become increasingly planar over a limited region (e.g. Halliday and Resnick 1974, Fig. 1). The wave fronts of a plane wave are parallel planes perpendicular to the direction of propagation of the wave; the rays are parallel lines normal to the wave fronts. Figure 2 shows wave fronts and rays of a plane wave propagating in the *x-z* plane at a velocity *V*; the propagation direction of the plane wave is at an angle θ to the *z*-axis.

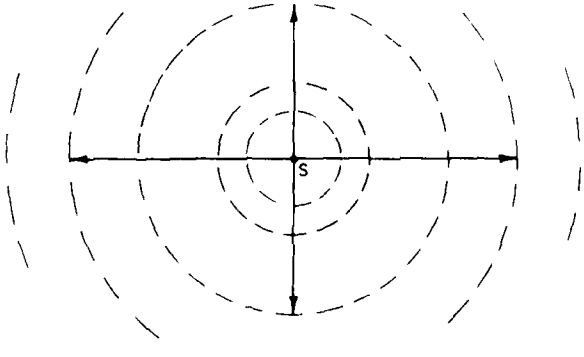

Figure 1. Wave fronts shown in two dimensions as dashed lines emanating from the point source, S. *Radial arrows normal to the wave fronts are rays. Each ray indicates the direction of propagation of the wave. The spherical wave fronts become locally planar as distance from* S *increases.*

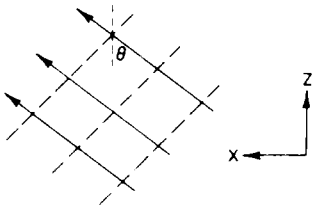

Figure 2. Wave fronts of a plane wave shown as dashed lines. Rays are shown as arrows.

The plane wave may be represented by the potential

$$\phi = A \exp i(k_x x + k_z z - \omega t) \tag{1}$$

where A is the amplitude of the wave potential; $k_x = k \sin\theta$ and $k_z = k \cos\theta$ are the horizontal and vertical components of the wave number (where $k = 2\pi/\lambda$ and λ is wavelength), $\omega = 2\pi/T = Vk$ is angular frequency and T is period.

In a homogeneous, isotropic, unbounded medium, the only waves that arrive at the receiver from an isotropic source are direct waves (Fig. 3a). In a homogeneous, isotropic half-space, surface-reflected waves (and Rayleigh waves) also arrive at the receiver (Fig. 3b). If velocities (α, β) increase uniformly with depth in the half-space, refracted waves arrive at the receiver after traveling minimum-time paths (Fig. 3c). If the medium consists of homogeneous layers of contrasting density and/or velocity, waves incident at an interface generate reflected waves and transmitted waves; which waves arrive at the receiver is determined by the angle of incidence and the number of times the waves are reflected (Fig. 3d).

A *P*-wave or a *SV*-wave that is incident obliquely at a planar boundary between two media in welded contact generates two reflected waves (*P*, *SV*) and two transmitted waves (*P*, *SV*). The angle at which each reflected or transmitted wave leaves the interface is determined by a generalized form of Snell's law. Figure 4 shows a *P*-wave ray in the *x*-*z* plane arriving at a planar boundary with an angle of incidence, $\theta_{P_{inc}}$. By Snell's law,

$$\frac{\sin\theta_{P_{inc}}}{\alpha_1} = \frac{\sin\theta_{P_{rfl}}}{\alpha_1} = \frac{\sin\theta_{S_{rfl}}}{\beta_1} = \frac{\sin\theta_{P_{rfr}}}{\alpha_2} = \frac{\sin\theta_{S_{rfr}}}{\beta_2} = \text{constant} \tag{2}$$

where *inc*, *rfl* and *rfr* denote incident, reflected and refracted (transmitted) waves, respectively. The constant is termed the ray parameter p. If a *SV*-wave in the *x*-*z* plane is incident at an angle $\theta_{S_{inc}}$, the governing equation is

$$\frac{\sin\theta_{S_{inc}}}{\beta_1} = \frac{\sin\theta_{S_{rfl}}}{\beta_1} = \frac{\sin\theta_{P_{rfl}}}{\alpha_1} = \frac{\sin\theta_{S_{rfr}}}{\beta_2} = \frac{\sin\theta_{P_{rfr}}}{\alpha_2} = \text{constant} \ . \tag{3}$$

A *SH*-wave in the *x*-*y* plane incident at the boundary does not generate *P*-waves or *SV*-waves because its motion is parallel to the boundary. Equations similar to eq 1 may be written for the compressional wave potential and the shear wave potential in each medium. The potentials are substituted in equations stating the continuity of stress and of displacement across the boundary; the set of equations is then solved for the coefficients of reflection and of transmission (refraction). Each coefficient is a ratio of amplitudes (of two potential equations) and depends upon the angle of incidence of the waves and on the elastic properties and densities of the media. Coefficients may be obtained also in terms of the amplitudes of displacement or energy. Graphs of

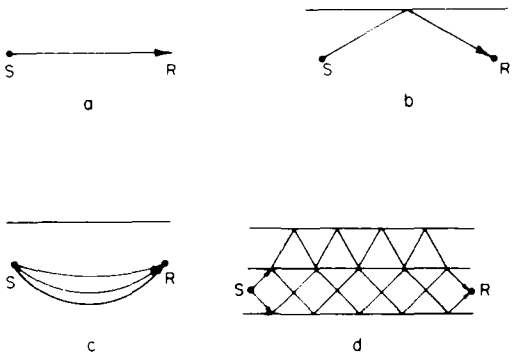

Figure 3. Wave types in bounded and unbounded media. S *denotes source,* R *denotes receiver.*

a. Direct wave in infinite, homogeneous medium.
b. Surface-reflected wave.
c. Refracted waves.
d. Multiply reflected waves in a layered medium.

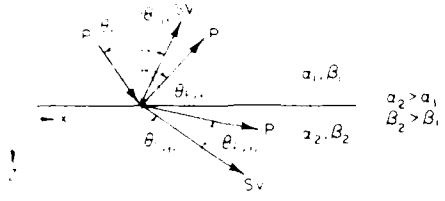

*Figure 4. Ray for each reflected (*P, S*) plane wave and each transmitted (*P, S*) plane wave generated by a plane* P*-wave incident at an angle $\theta_{P_{inc}}$ at a planar boundary. The* P*- and* S*-wave velocities are α_1 and β_1 in medium 1 and α_2 and β_2 in medium 2.*

transmission and reflection coefficients as a function of angle of incidence (for various density and velocity contrasts) are given in Grant and West (1965, pp. 57–59) and Telford et al. (1978, p. 254).

As the angle of incidence of the *P*-wave increases from $\theta_{P_{inc}} = 0$, the angle of refraction of the transmitted *P*-wave also increases (eq 2). When $\theta_{P_{inc}} = \sin^{-1}(\alpha_1/\alpha_2)$, $\theta_{P_{rfr}} = 90°$ and the transmitted *P*-wave propagates in medium 2 at grazing incidence; $\theta_{P_{inc}}$ is termed the critical angle ($\theta_{P_{crit}}$) for refraction of the *P*-wave and the refracted wave is termed the head wave. The analysis of head waves is based upon the theory of curved wave fronts at a planar interface (or plane waves incident at curved interfaces). The reflected *P*-wave energy is maximum at $\theta_{P_{inc}} = \theta_{P_{crit}}$ because this is the condition for total internal reflection.

When $\theta_{P_{inc}} > \theta_{P_{crit}}$, Snell's law would require $(\alpha_2/\alpha_1)\sin\theta_{P_{inc}}$ be greater than 1. In this case, $\theta_{P_{rfr}}$ is taken to be complex, $\theta_{P_{rfr}} = \pi/2 - i\delta$ and $\delta = \cosh^{-1}[(\alpha_2/\alpha_1)\sin\theta_{P_{inc}}]$ (Grant and West 1965, p. 66). When $\theta_{P_{rfr}}$ is substituted in a potential equation for the transmitted *P*-wave, the equation that results has the form

$$\Phi_{P_{rfr}} = B \exp\left[i \frac{\omega}{\alpha_t} \sin\theta_{P_{inc}} (x + zf)\right] ,$$

where

$$f = \sqrt{(\alpha_1/\alpha_2)^2 \csc^2 \theta_{P_{inc}} - 1}$$

is an imaginary number. Therefore, the transmitted *P*-wave as expressed by $\Phi_{P_{rfr}}$ is not an ordinary *P*-wave, but rather is an inhomogeneous wave characterized by an exponential decrease in amplitude with vertical distance from the interface. In terms of the ray parameter, the transmitted *P*-wave is an inhomogeneous wave when $p > 1/\alpha_2$. If $\beta_2 < \alpha_1$, a *P*-wave incident at an angle of $\theta_{P_{inc}} > \theta_{P_{crit}}$ generates a transmitted *SV*-wave at a real angle of refraction and so the *SV*-wave propagates away from the boundary. If $\beta_2 > \alpha_1$, there is a critical angle for refraction of the *SV*-wave. When $\theta_{P_{inc}} = \theta_{SV_{crit}} = \sin^{-1}(\alpha_1/\beta_2)$, the *SV*-wave generated by the incident *P*-wave is a head wave. If $\theta_{P_{inc}} > \theta_{SV_{crit}}$, the angle of refraction of the *SV*-wave is complex and the transmitted *SV*-wave is an inhomogeneous wave. Both *P* and *SV* transmitted motion are trapped at the interface.

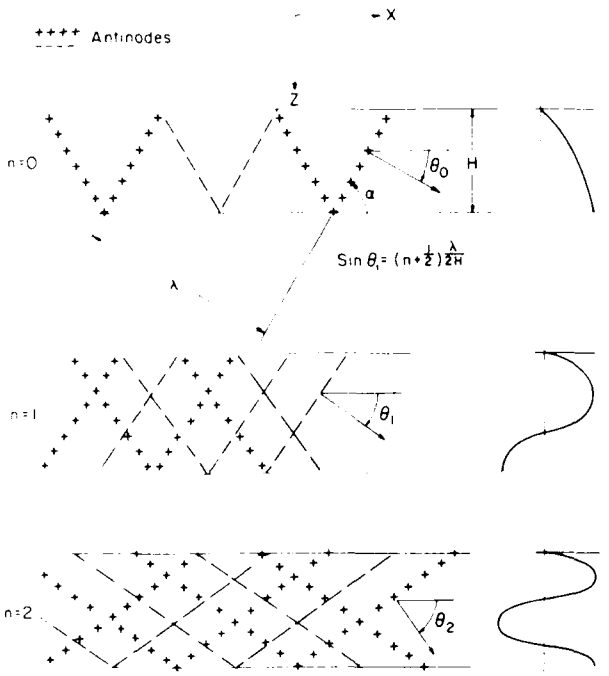

Figure 11. Plane wave representation of normal modes of the first three orders. The boundary conditions are a pressure-released surface and a pressure-reinforcement (rigid) bottom (adapted from Urick 1979).

decay with range. If the imaginary part of the complex wave number is much smaller than the real part, then the real part is used in determining phase velocity ($C = V/\sin\gamma_n = \omega/k_n$) and group velocity ($U = d\omega/dk_n$), while the imaginary part is a damping coefficient (Brekhovskikh 1960, p. 405). Reflection coefficients that are dependent on γ are used when the waveguide boundaries are not perfect reflectors.

The approach used above to determine the condition for constructive interference of plane waves in a homogeneous waveguide can be applied in the case of a layered waveguide (velocity dependent on depth within waveguide). This requires that the effect of partial reflection at the layer interfaces on the phase of each plane wave and on the energy content of the plane waves be incorporated in the solution.

Normal modes that have *SH* polarization are Love waves, which are specified by their mode number ($n = 0, 1, 2, \ldots$). The fundamental normal mode with *SV* polarization corresponds to the dispersive Rayleigh wave and is designed as the Rayleigh mode; the higher order modes are designated as the first, second, etc., *SV* mode (Grant and West 1965).

There are many computer programs available to obtain normal mode solutions to underwater wave propagation problems, some of which are useful in solid earth studies. The normal mode solution can be obtained by solving the Helmholtz equation; this is a time-independent wave equation that results when the pressure field is assumed to be of constant angular frequency, $P = S(r,z) \exp(-i\omega t)$. If the spatial factor has the form $S = H_0^{(1)}(k_0 r) f(r, z)$ and the asymptotic approximation of the Hankel function (valid for $k_0 r >> 1$) is substituted, then the Helmholtz equation that results (in cylindrical coordinates) is

$$\frac{\partial^2 f}{\partial z^2} + \frac{\partial^2 f}{\partial r^2} + 2ik_0 \frac{\partial f}{\partial r} + (k^2 - K_0^2) f = 0$$

(nodes), the lines of positive signs are wave fronts of positive wave amplitude, and the lines of negative signs are wave fronts of negative amplitude. Each wave front impinges on the waveguide boundaries at an angle γ. In order for superimposed plane waves to interfere constructively, the phase difference between the waves must be an integral multiple of 2π ($2n\pi$, $n = 0, 1, 2, \ldots$). This requirement leads to a relationship between thickness of the waveguide, angle of incidence of the plane waves, and frequency. Only waves of certain frequencies will interfere constructively and give rise to a standing wave pattern in the z-direction; frequency is uniquely determined when mode number (n) and γ are specified. The apparent velocity (velocity in the x-direction) of the plane waves is $C = V/\sin\gamma$; this relationship is used to rewrite the equation for constructive interference in terms of C instead of γ. The result is a dispersion equation (phase velocity-frequency relation) for each normal mode.

Since a critical angle of incidence exists for the retention of wave energy in the waveguide by total internal reflection, there is a cutoff frequency for each normal mode. At frequencies below the cutoff frequency, the normal modes are attenuated as they propagate even in a lossless medium due to the transmission of wave energy across the waveguide boundary (leaky modes). The energy lost from the waveguide as transmitted waves may be returned by reflections at depth and so, over short ranges, may contribute to the wave field at the receiver.

This treatment of normal modes requires that the wave energy has propagated sufficiently far from the source for the representation of normal modes as interfering plane waves to be valid. The reflection coefficient for spherical waves is the sum of the plane-wave reflection coefficient and a correction term that goes to zero at very high frequencies. The correction term is negligible when source and receiver are located at distances from the waveguide boundary that are large relative to wavelength (Brekhovskikh 1980, p. 247; Clay and Medwin 1977, p. 64). In a mathematical derivation of the normal mode solution, the asymptotic representation of the Hankel function is substituted for the function itself, which is valid for distances from the source that are large relative to wavelength.

The normal mode solution for the relatively simple case of a fluid layer over a rigid half-space (Fig. 10) is given here as an example of the solution format. (The case of a solid layer over a rigid bottom is more complex because two types of waves are present [P, S] and so two potentials are required to express the normal mode solution. If the half-space is nonrigid, a solution must be found for that region as well, e.g. that of Ewing et al. 1957, p. 138.) The potential ϕ for horizontally propagating waves in the layer is

$$\phi = \Sigma B_n \left[R_1(\gamma_n)\exp(-ikz\cos\gamma_n) + \exp(ikz\cos\gamma_n)\right]\exp(ikx\sin\gamma_n) \qquad (13)$$

(Brekhovskikh 1960, p. 407), where n designates a particular normal mode, R_1 is the reflection coefficient for waves incident from above at the lower boundary of the waveguide, and the coefficient B_n, which is a function of the position and strength of the source, determines the degree of excitation of each normal mode. The z-dependence of the amplitude of each normal mode is determined by the expression in the brackets of eq 13. The potential ϕ is the sum of potentials for the upgoing (ϕ_-) and downgoing (ϕ_+) plane waves where $\phi_- = A\exp[i(-k_z z + k_x x)]$, $\phi_+ = B\exp[i(k_z z + k_x x)]$, $k_x = k\sin\gamma$, and $k_z = k\cos\gamma$. An equivalent equation could be written in terms of the coefficient A and the reflection coefficient for waves incident from below at the upper boundary of the waveguide, R_2. The potential ϕ (eq 13) satisfies the equation $R_1 R_2 \exp(2ik_z H) = 1$. Examples of plane waves at three angles of incidence and the normal modes that result from constructive interference are given in Figure 11. For a given frequency, a higher order mode corresponds to a steeper ray path.

The normal mode solution to the wave equation can be generalized to include attenuation due to propagation in an imperfectly elastic (lossy) medium and imperfect reflections at the waveguide boundaries; this is done by making the wave number complex and so introducing an exponential

Consider a homogeneous elastic layer of thickness H over a homogeneous half-space, each with shear wave velocity (β) and density (ρ) as shown in Figure 8. The dispersion equation for Love waves is

$$\tan\left(\frac{\omega H}{c}\sqrt{c^2/\beta_1^2 - 1}\right) = \frac{\mu_2\sqrt{1 - (c^2/\beta_2^2)}}{\mu_1\sqrt{(c^2/\beta_1^2 - 1)}} \quad ; \tag{12}$$

its solution is graphed in Figure 9. The cutoff frequency is zero for the fundamental mode ($n = 0$) and

$$\omega_{cn} = \frac{n\pi\beta_1}{H} / (1 - \frac{\beta_1^2}{\beta_2^2})^{1/2}$$

for the higher modes ($n > 0$) (Aki and Richards 1980, p. 264). For a given mode, the phase velocity is equal to β_2 at the cutoff frequency and is equal to β_1 in the limit of $\omega \to \infty$ (asymptotic solution to eq 12). This is physically reasonable in that high frequency waves (short wavelengths) are confined to the vicinity of the layer surface whereas low frequency waves (long wavelengths) penetrate the deeper, high velocity medium and are little affected by a relatively thin surface layer. A dispersion relation for Rayleigh waves is more complicated. Pilant (1979), Takeuchi and Saito (1972), and Aki and Richards (1980) treat Rayleigh wave propagation in a layered medium. Equations 11a, b indicate that Rayleigh waves are retrograde elliptical at the surface and prograde elliptical below the nodal plane. Results of computer calculations of surface wave dispersion indicate that higher order modes are prograde elliptical at the surface.

The characterization of Rayleigh waves and Love waves in terms of modes indicates a relationship between surface waves and normal modes; the relationship will become apparent in the discussion of normal mode theory in the next section. Here, it should be noted that certain conditions must be satisfied if the approach of modeling surface waves as plane waves that are multiply reflected in a layer is to be valid. The use of plane waves requires that the waves have propagated sufficiently far from the source to be well represented as planar rather than spherical or cylindrical. This condition is expressed in terms of the layer thickness: the distance from the source must be large in terms of the layer thickness (Grant and West 1965, p. 77).

SECTION 5. NORMAL MODES

A discussion of normal modes is given in Ewing et al. (1957), Grant and West (1965), Officer (1974), and Brekhovskikh (1980). The propagation of normal modes can be represented as arising from the interference of plane waves that are multiply reflected at the boundaries of the waveguide. One set of reflected waves in an elastic waveguide with plane, parallel boundaries overlying a rigid half-space is shown in Figure 10. The solid lines are wave fronts of zero amplitude of the waves

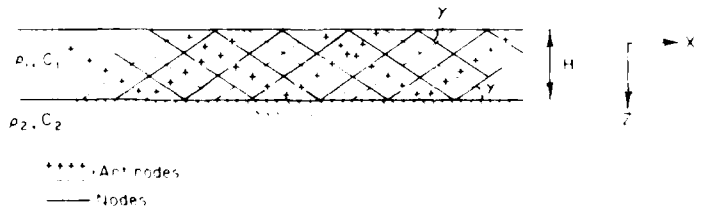

Figure 10. Wave fronts impinging on boundaries of waveguide at angle γ (adapted from Urick 1983).

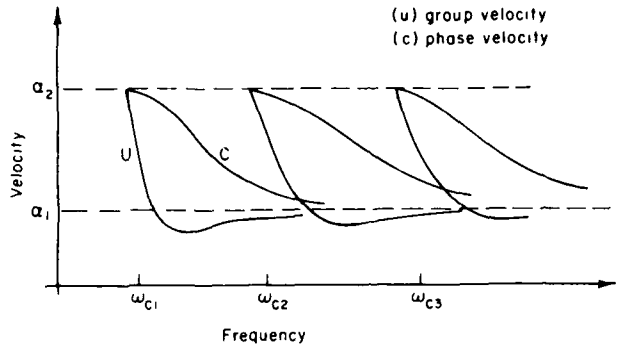

Figure 7. Dispersion curves for three modes (1, 2, 3). The cutoff frequencies are ω_{c1}, ω_{c2}, and ω_{c3}, respectively. The curves are drawn for the situation of increasing seismic velocity with depth (adapted from Officer 1974).

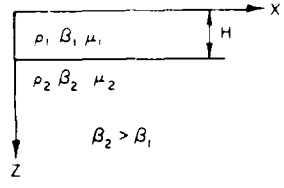

Figure 8. Geologic model for which the dispersion equation for Love waves (eq 12) is calculated.

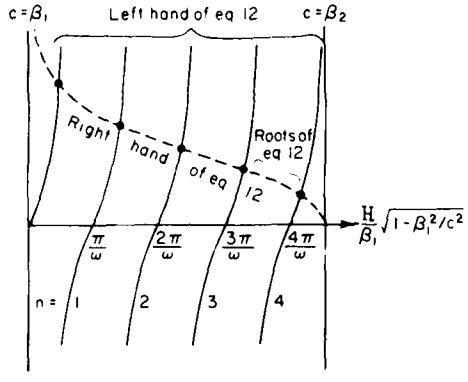

Figure 9. Graphic solution of eq 12 for the dispersion of Love waves in a single layer over a half-space. Each side of eq 12 is plotted as a function of $H[1-(\beta_1^2/C^2)]^{1/2}/\beta_1$ (adapted from Aki and Richards 1980).

Surface waves propagating in a layer can be viewed as arising from the interference of plane waves that are multiply reflected at the boundaries of the layer. The condition for constructive interference of the plane waves leads to the development of a dispersion equation that expresses the frequency-velocity relation of solutions to the wave equation in terms of the thickness of the layer, the velocities and densities of the layer and substratum, and the angle of incidence of the plane waves. The dispersion equation is multivalued due to a tangent function; one dispersion curve is obtained for each mode (value of n, where $n = 0, 1, 2, \ldots$, each corresponding to a range of the tangent function) specified. There is a cutoff frequency ω_{cn} for all but the fundamental ($n = 0$) Love mode and for all modes in a layered acoustic medium. At frequencies equal to or greater than the cutoff frequency, surface waves propagate horizontally with essentially no attenuation in a lossless medium but do decay exponentially with depth; at frequencies below the cutoff frequency, the wave attenuates as it propagates even in a lossless medium due to the radiation of energy across the layer boundary (leaky modes) as well as decaying exponentially with depth. The cutoff frequency increases with mode number so there is a finite number of modes possible at a given frequency. The phase velocity (c) is the velocity at which a point of a particular wave is propagating. The group velocity (U) is the velocity at which the energy associated with a particular frequency group travels. Group and phase velocity are related by $U = c - \lambda(dc/d\lambda)$. A generalized example of dispersion curves for phase velocity and group velocity is given in Figure 7.

and

$$\psi = \mathbf{B} \exp i\omega [t - (x/c) + bz] . \tag{9}$$

The amplitude coefficient **B** must be directed in the y-direction, so eq 9 is rewritten as

$$\psi_y = B \exp i\omega [t - (x/c) + bz] . \tag{10}$$

Substitution of eq 8 and 10 in the wave equation ($\partial^2/\partial t^2 = v^2(\partial^2/\partial x^2)$, $v = \alpha$ or β) leads to $a^2 = 1/\alpha^2 - 1/c^2$ and $b^2 = 1/\beta^2 - 1/c^2$. If $c > \alpha > \beta$, a and b are real and ϕ and ψ_y represent two waves propagating in oblique directions that do not decay with depth. In order to obtain a representation for waves that are restricted to the vicinity of the surface, it must be that $c < \alpha$ and $c < \beta$ so that a and b are imaginary. By choosing the imaginary parts of a and b to be positive ($a = i\sqrt{1/c^2 - 1/\alpha^2}$, $b = i\sqrt{1/c^2 - 1/\beta^2}$), the waves will decay exponentially with depth as they propagate. The system of equations that results from application of the boundary conditions $\sigma_{zz} = \sigma_{xz} = 0$ is solved for c; for a Poisson's solid (medium with Poisson's ratio of ¼), $c = C_r = 0.9194\beta$. The displacement vector **u** for Rayleigh waves has scalar components:

$$u_x = M \exp i\omega \left(t - \frac{x}{c}\right) (e^{-0.8475\omega z/c} - 0.5773e^{-0.3933\omega z/c}) \tag{11a}$$

$$u_z = -iM \exp i\omega \left(t - \frac{x}{c}\right) \cdot (-0.8475e^{-0.8475\omega z/c} + 1.4679e^{-0.3933\omega z/c}) . \tag{11b}$$

These equations show that a surface wave of low frequency decays more slowly than one of high frequency. At the surface, $u_z/u_x = 1.468$ and at a depth of 0.193λ, $u_x = 0$ (Kolsky 1953, p. 20-21). A specific Poisson's ratio has been substituted in the general equations in order to make the equations given here more tractable; alternately, Grant and West (1965, Fig. 3-10) show $u_z/u_x\big|_{z=0}$ and the depth to the nodal layer as a function of Poisson's ratio.

In a similar manner, the displacements due to a Love wave propagating in an elastic layer over a half-space are $u_y = A \exp i\omega (t - (x/c) + b_1 z) + B \exp i\omega (t - (x/c) - b_1 z)$ in the layer and $u_y = C \exp i\omega (t - (x/c) + b_2 z)$ in the half-space, with $b_1 = \sqrt{1/\beta_1^2 - 1/c^2}$ and $b_2 = i\sqrt{1/c^2 - 1/\beta_2^2}$. The boundary conditions are continuity of stress and displacement at the layer/half-space interface and the vanishing of the stress at the free surface. The equation that results upon elimination of A, B, and C is the dispersion equation, expressing the dependence of velocity of propagation on frequency.

The treatment of surface waves can be generalized to the case of several layers over a half-space. In each layer there are upward and downward propagating (and decaying) waves that interfere; only downward propagating (and decaying) waves exist in the half space. Long wavelength waves penetrate the medium more deeply and so have a phase velocity that is an average of the medium properties to a greater depth. Boundary conditions on motion within the vertically inhomogeneous medium are continuity of stress and displacement across the layer interfaces. In order to construct a dispersion equation for the multi-layered medium, the motion at a subsurface layer must be related to motion at the surface; the equations expressing this relation can be solved by numerical integration (e.g. Runge-Kutta method) or by matrix techniques (e.g. Thomson-Haskell method) (Aki and Richards 1980, p. 270). Phase velocity-frequency curves are constructed from the dispersion relation; a comparison of the curves and field data indicates how accurately the model used to construct the curves represents the velocity profile and near-surface structure of the earth.

Hermann (1978) gives annotated computer programs for surface wave seismology. A combination of programs supplied will 1) solve for phase and group velocities as a function of period for Love and Rayleigh waves in a multi-layered medium, 2) calculate the Rayleigh wave and Love wave displacements in the layers, and 3) generate synthetic seismograms.

the computational advantages of evaluating the frequency integral first and then integrating over real values of the ray parameter (or slowness). Using Chapman's approach, Dey-Sarkar and Chapman (1978) obtain the following displacement equation valid for ($\omega pr\Delta >> 1$):

$$u(t, \Delta, r) \simeq - \frac{\ddot{m}(t)}{\pi(2r_s \sin\Delta)^{1/2}} * Im[\Lambda(t) * \sum_{t=\theta} \frac{p^{1/2} C(p)}{4\pi\alpha_s^2 (p_s q_s p_r q_r)^{1/2}} (\frac{p}{q_r}) \frac{1}{|\theta'|}]$$

where r = radius

r, s = receiver radius and the source radius, respectively

$m(t)$ = the source term

$C(p)$ = the product of all reflection and transmission coefficients defining the ray

$\Lambda(t)$ = a time series

q = a function of ray parameter p and radius

$\theta(p) = pr\Delta + \tau(p)$

$\tau(p)$ = the intercept function obtained from a graph of travel time vs range

Δ = the angular separation between source and receiver measured from the center of the earth.

The summation is over all real solutions of $t = \theta(p)$.

Choy et al. (1980) compare synthetic seismograms generated by the reflectivity method and by full wave theory. An advantage of the full wave theory method is that no truncation phase is present in the seismograms, while integration over a limited range of angles of incidence causes a truncation phase to be present in the reflectivity seismograms; a disadvantage is that the rays must be specified in order to be included in the full wave theory calculations (unlike the reflectivity method in which all internal multiples and conversions are automatically included).

SECTION 4. SURFACE WAVES

Surface waves exist in the near-surface region of a medium having a free surface. They decay exponentially with depth in the medium but attenuate laterally with a $1/(\text{range})^{1/2}$ dependence. The types of surface waves are distinguished by differences in particle motion and in conditions for occurrence. Love waves are *SH*-waves that propagate in a layered medium. Rayleigh waves are coupled *P-SV* waves that propagate in a layered medium and at the surface of a half-space. In the case of a single layer over a half-space, Love waves exist only when the shear velocity in the layer is less than that of the half-space. Love waves can exist in a multi-layered medium in which velocity generally increases with depth, i.e. even if local low velocity layers are present (Pilant 1979, p. 161; Ewing et al. 1957, p. 224). Rayleigh waves propagate without dispersion at the surface of a half-space and, like Love waves, with dispersion in a layered medium. However, in the case of a layer (shear velocity β_1) of thickness H over a half-space, the Rayleigh waves are not dispersed but rather propagate with a velocity of $C_r \approx 0.92\beta_1$ if $\lambda << H$ for all wavelengths (Press and Ewing 1950).

The nature of Rayleigh waves is evident in the derivation of the displacement equations for waves propagating along the surface of an elastic half-space. The displacement vector for a propagating wave is **u**. A property of vectors is that any vector can be written as the sum of a gradient and a curl; therefore, **u** = **v** + **w** where **v** = **grad** ϕ and **w** = **curl** ψ. The potentials ϕ and ψ can be expressed in general terms as*

$$\phi = A \exp i\omega [t - (x/c) + az] \qquad (8)$$

*E.A. Okal, Yale University, personal communication, 1979.

are considered; layers $j > m$ compose the reflecting zone for which the complete complex reflectivity is $R_{pp}(\omega, \gamma)$; $v_1 = \sqrt{k_{\alpha_1}^2 - k_{\alpha_m}^2 \sin^2 \gamma}$; and range Δ is the angular separation between source and receiver positions measured from the center of the earth (horizontal range at the surface is $x = 0.017\ \Delta r_e$ where r_e is the radius of the earth.

In evaluating displacement with this method, a Bessel function typically is replaced by its asymptotic approximation for large arguments; this is valid for large source-receiver distances or large horizontal wave numbers, i.e. high frequencies. The integration is usually carried out over a limited range (due to computational costs) of real ray parameters. The use of real ray parameters restricts the method to body waves; the use of a limited range of ray parameters introduces a truncation phase in the seismogram. The range of ray parameters corresponds to an equally restricted range of angles of incidence; in the case of a deep reflecting-refracting zone, horizontally traveling energy is left out of the computation. If the top of the reflecting-refracting zone is at the surface, horizontally traveling energy contained in reflected and refracted waves as well as surface wave energy should be included in the computation.

Burdick and Orcutt (1979), in a comparison of the reflectivity and generalized ray methods, cite the approximations customarily made and reference papers in which such approximations are not made in obtaining a solution. Sato and Hirata (1980) evaluate results obtained with these methods and with a third hybrid method having characteristics of both.

An approach similar to the reflectivity method is given by Kennett (1979, 1983) for plane waves from a surface source that are multiply reflected during propagation in a multi-layered medium; effects of excluding converted shear waves and free surface reflections and of including attenuation are shown.

The final wave theory considered is full wave theory. This is actually a term that applies to several theories. The only distinction among the theories given here is that one approach to a full wave theory of body wave propagation results in the calculation of the WKBJ seismogram.

WKBJ theory refers to a method of finding approximate solutions to a second-order differential equation. When the method is applied to the wave equation, it results eventually in the WKBJ seismogram. Several approximations are made in the process of obtaining the WKBJ solution, one of which is to retain only the first two terms of a binomial expansion. As a consequence of the approximations, the solution is valid for frequencies that are large in relation to velocity gradients or equivalently, for a nearly homogeneous medium. Grant and West (1965) show the equivalence between this asymptotic solution to the wave equation and the approximate solution obtained by means of the eikonal equation, both of which involve the propagation of wave fronts along paths that are determined by Snell's law. The WKBJ method cannot handle the situation of a turning point, i.e. when the ray has reached its maximum penetration depth and is directed horizontally prior to turning toward the surface, due to a singularity that arises from the use of the truncated binomial expansion. A different method, such as an Airy function, is used in the vicinity of the turning point. The solutions obtained are oscillatory above the turning point and exponentially decaying below the turning point.

The full wave theory (Aki and Richards 1980, Choy et al. 1980) is applicable to body wave propagation in situations involving radial inhomogeneity, smoothly varying density and velocity, ray paths with turning points (including those near grazing incidence at an interface), critically incident rays, caustics, wave interference due to multipathing, and non-ray theoretical effects such as diffraction. As a result of the first two characteristics, a realistic earth model can be used, rather than a representation of planar layers of constant velocity and density. The great versatility of the full wave theory results from the incorporation of the frequency dependence of the waves. The equation for radial displacement is integrated in the real frequency domain and in the ray parameter domain; depending on the path of integration in the ray parameter domain, the displacement equation reduces to the solution obtained from ray theory if the reflection and refraction coefficients are assumed to be independent of frequency. Chapman (1978) has investigated

with amplitudes lower than a preselected percentage of the maximum amplitude of the first arrivals can be excluded from the seismogram. Krebes and Hron (1981) show that there is good agreement between synthetic seismograms obtained using asymptotic ray theory and those obtained using the Thomson-Haskell matrix method in the case of anelastic media. The method can be used with laterally varying structures (McMechan and Mooney 1980) provided that the rays can be traced through the structure.

Quantized ray theory (Wiggins and Madrid 1974) and subsequently disk ray theory (Wiggins 1976) were developed as modifications of asymptotic ray theory to obtain more accurate body wave amplitudes. Examples of synthetic seismograms obtained with the disk ray method for models of laterally heterogeneous elastic and anelastic media are given by Braile et al. (1983).

The third wave theory considered is the reflectivity method (Fuchs 1968; Fuchs and Müller 1971; Aki and Richards 1980, p. 393-404). It is used to study the reflection and refraction (including critical refraction) of spherical waves incident on and propagating within a zone of layers with planar interfaces. The method is customarily applied to body wave problems but can incorporate surface waves. It involves the determination of the progressive partitioning of wave energy due to one or multiple reflections of each wave considered together with phase changes (delays) due to the propagation of the wave through each layer. The layered zone in which reflections and refractions of interest occur can be located at the surface (Fertig and Müller 1978) or buried; in the latter case, waves from a source position may be propagated to the reflecting-refracting zone and returned from the zone to the receiver position by considering only the occurrence of refraction (Fuchs and Müller 1971, Aki and Richards 1980) or reflection and conversion of waves propagating in the surface region (Kohketsu 1981). An equation for displacement at the receiver position is obtained after two integrations, the first in the domain of the wave number (k), ray parameter ($p = k/\omega$) or angle of incidence and the second in the frequency (ω) domain. The reflectivity term in the displacement equation is the exact sum of the infinite series of reflections for all possible multiply reflected waves (including converted waves) within the reflecting-refracting zone (Aki and Richards 1980, p. 402). Accordingly, the solution obtained with the reflectivity method is equivalent to the net displacement due to the arrival of an infinite number of generalized rays.

The compressional potential obtained from the reflectivity theory for the case of a point source at the surface of a plane layered earth is

$$\phi(\omega, \Delta) = F(\omega) \int_{\gamma_1}^{\gamma_2} k_{\alpha_m} \frac{\sin\gamma \cos\gamma}{i v_1} \left[\frac{1}{\sqrt{2\pi \Delta k_{\alpha_m} \sin\gamma}} \cdot \exp\left(-i\left(\Delta k_{\alpha_m} \sin\gamma - \frac{\pi}{4}\right)\right)\right]$$

$$\cdot T(\omega, \gamma) \cdot R_{pp}(\omega, \gamma) \exp(-i\tau)\, d\gamma$$

(Burdick and Orcutt 1979) where

$F(\omega)$ = the Fourier-transformed source time function
γ = angle of incidence in the mth layer
$k_{\alpha_j} = \omega/\alpha_j$.

The index j refers to the jth layer; layers $j = 1, 2 \ldots, m$ compose the refracting zone in which only the transmission losses $T(\omega, \gamma)$ and the phase shifts $\tau(\omega, \gamma)$ of a plane wave at constant γ and ω

in order to reduce computational time; here τ is the travel time of the ray with ray parameter p and the potential equation is

$$\phi(r, z, t) = \frac{1}{4\pi\sigma} \cdot \frac{1}{R} \cdot H(t - \frac{R}{\alpha}),$$

where $R = \sqrt{r^2 + z^2}$. Similar equations for transmitted waves and reflected waves in a layered medium involve the potential transmission coefficient and the potential reflection coefficient, respectively, and an R term that is dependent on the location of the source relative to the layer boundaries.

The displacement field at the receiver position is determined by summing in the time domain the contributions of rays that travel from the source to that point. Each reflection or transmission of a ray at a layer interface is taken into account as it proceeds from source to receiver. Computational cost may impose a limit on the number of rays included in the construction of the seismogram. A first attempt is to use only the rays that are reflected once between source and receiver; the number of such rays depends on the number of layers used to model the velocity profile of the medium. As multiply reflected rays of increasing order are included in the computations, the synthetic seismogram changes until eventually inclusion of additional rays does not further change the character of the seismogram. For a medium composed of thin layers, the number of rays that must be included for accuracy is high; in this case, truncation of the infinite series of multiple reflections can introduce serious errors. The multiples that must be included are specific to the problem and depend on the depth and thickness of the reflected layers, the velocity and density contrasts at interfaces, and the source-receiver separation. The validity of the synthetic seismogram generated depends upon the incorporation of all necessary rays. The solution is more difficult to obtain if attenuation is incorporated in the problem.

The second wave theory considered is asymptotic ray theory (Hron and Kanasewich 1971, Pilant 1979). This approach represents the displacement due to propagation of a plane wave in a layered medium as the sum of an infinite series of products involving a spatially dependent amplitude and two frequency terms, one an exponential and one a power series in inverse frequency,

$$u(x, y, z, t) = \sum_{n=0}^{\infty} A_n(x, y, z) \frac{e^{i\omega(t-T)}}{(i\omega)^n} \quad ;$$

here T is a phase function that depends upon the ray path. The result is an asymptotic solution to the wave equation that has characteristics of geometrical ray theory. In the limit of high frequencies, a useful asymptotic solution is obtained with only one or two terms retained. If only the first term (n=0) of the series is retained, the displacement equation is the same as the solution to the eikonal equation (eq 4) and the results obtained are necessarily identical with those due to geometrical ray theory for wave propagation in a plane-layered medium. Higher-order, frequency-dependent terms are used in problems involving diffraction phenomena, curved interfaces, and inhomogeneous media; the n=1 term is necessary in the case of head waves.

Hron et al. (1974) give examples of synthetic seismograms generated by the asymptotic ray method for the case of a compressional plane wave impinging on a plane-layered medium and a surface source. Each ray is specified by the number of linear segments composing it and the number of conversions that occur. An advantage of this method is that each constitutent ray (or group of kinematic rays) of the synthetic seismogram can be identified. The amplitude of each ray is determined using plane wave coefficients of reflection and transmission; the use of frequency-independent coefficients is justified by the use of zero-order terms (high frequency approximation). Geometrical spreading, neglected here because the source is assumed to be at infinity, is normally incorporated in the ray amplitude formulation (McMechan and Mooney 1980). Rays

formed by the intersection of rays) with finite amplitudes rather than the infinite amplitudes that ray theory predicts, and the interference of waves that travel different paths but have similar arrival times (multipathing). The requirement concerning velocity changes ($\lambda_0 (\delta C'/C) << 1$) is satisfied if the wave is of sufficiently short wavelength (high frequency approximation) or if abrupt velocity changes in the actual velocity profile are replaced by layered transition zones of constant velocity in which the thickness of the layers is such that the requirement is not violated, *i.e.* thickness/wavelength > 10 (or even 100). The requirement concerning changes in curvature of the wave front ($\lambda_0 \delta W'' << 1$), which again is satisfied in the limit of high frequencies, limits the validity of the ray theory approach to plane waves; this requirement is a restriction to the far-field region such that spherical waves have traveled far enough from the source so as to appear as plane waves. The far-field condition requires that the horizontal source-receiver separation be equal to several wavelengths.

Wave theory

There are several methods of generating synthetic seismograms that are based upon wave theory. In each case, the wave theory can be shown to encompass geometrical ray theory. A significant difference between ray theory and wave theory, which often also formulates its development in terms of rays, is that wave theory incorporates a dependence on the frequency of the seismic wave in its solution.

The first wave theory considered is generalized ray theory, also known as exact ray theory, the method of generalized reflection and transmission coefficients (Müller 1970) or the Cagniard-de Hoop method (Aki and Richards, 1980, 224-253, 386-393). It is applicable to problems involving spherical waves incident on planar interfaces and can incorporate direct waves, reflected waves, critically refracted waves and Rayleigh waves in the solution. It requires an integration in the complex ray parameter plane and a Laplace transform to obtain solutions in the time domain; the path of integration is different for each generalized ray and must be found exactly. In Laplace space, the compressional potential due to a point source in a homogeneous medium is†

$$\Phi(r, z, s) = \frac{sG(s)}{2\pi^2 \sigma} \cdot Im \int_0^{i\infty} \frac{p}{\eta_\alpha} K_0(spr) e^{-s\eta_\alpha |z|} dp,$$

where p = the complex wave parameter
s = an imaginary parameter analogous to the frequency of a wave ($p = \gamma/s$, where γ is analogous to a radial wave number)
$\sigma = \lambda + 2\mu$
$\eta_\alpha = (1/\alpha^2 - p^2)^{1/2}$
G = Green's function
K_0 = the modified Bessel function.

No approximations need be made in obtaining the solution. If Bessel's function is replaced by the first term of its asymptotic expansion, the expression for ϕ in the time domain that results is

$$\phi(r, z, t) = \frac{1}{\sqrt{t}} * \left[\frac{1}{\sigma} \frac{1}{\sqrt{8\pi^3 r}} \cdot Re[\sqrt{p(t)}] \frac{H(t-R/\alpha)}{\sqrt{t^2 - R^2/\alpha^2}}\right],$$

where H is the Heaviside function and * denotes convolution†. The first-motion approximation $(t-\tau + 2pr)^{1/2} \approx (2pr)^{1/2}$, which is valid for large ranges (r) but fails at long times (t), is often made

† E.A. Okal, Yale University, personal communication, 1980.

i. e. when $\sin\theta = 1$; this is the penetration depth of the ray which then turns upward. The time required for the ray to travel from depth Z_0 to depth Z_f is given by

$$t_f - t_0 = \int_{Z_0}^{Z_f} \frac{dZ}{C(Z)[1 - p^2C^2(Z)]^{\frac{1}{2}}} \quad . \tag{6}$$

The horizontal (surface) component of the ray path at a depth Z_f is

$$X_f - X_0 = \int_{Z_0}^{Z_f} \frac{p\,C(Z)\,dZ}{[1 - p^2C^2(Z)]^{\frac{1}{2}}} \quad . \tag{7}$$

If the ray reaches Z_p then the integration of eq 6 and 7 must be performed twice, once for the downgoing ray path and once for the upgoing ray path. The accuracy of all the calculations depends both on the approximations of ray theory stated above and on the velocity function $C(Z)$ used to approximate the actual variation of velocity with depth. Greenhalgh and King (1981) give the ray equations that are valid for various velocity-depth functions. Also, the equations were derived for the case of a flat earth that is homogeneous or is inhomogeneous with depth only. The approximation of a flat earth is justified in wave propagation problems involving source-receiver separations small enough that the curvature of the earth may be neglected. Officer (1974) derives equivalent equations for the case of a spherically stratified earth; for this case, the quantity that is constant along the ray is $r \sin\theta/C$, which is also called the ray parameter, where r is the radial distance from the center of the earth.

Shadow zones exist when the velocity profile is such that rays are directed away from a particular region; this occurs when a trend of gradually increasing velocity with depth is interrupted by a negative velocity gradient (velocity decreases with depth) and then resumed. Similarly, convergence of rays occurs when the velocity profile is such that rays cross and become focused in a region; in this case, a trend of gradually increasing velocity with depth is interrupted by a greater positive velocity gradient and then resumed. A complete discussion of variation in the location and energy content of rays arriving at the surface due to different velocity profiles is given in Officer (1974).

The path that a given ray travels through a medium can be determined by ray tracing; this requires specifying the takeoff angle (the orientation at which the ray leaves the source) and the velocity profile through the medium and then applying Snell's law sequentially. Repeating this process for a range of takeoff angles leads to identification of locations at which wave energy arrives at the surface, as well as focusing and defocusing of the energy. The converse problem, determining what rays from a known source arrive at a given surface location, is more difficult and involves an iterative process beginning with a trial solution. In the shooting method, the initial orientation of the ray is specified and subsequently adjusted until the ray arrives acceptably close to the receiver location; in the bending method, the source and receiver positions are specified and the ray path is adjusted (Aki and Richards 1980, p. 727). Procedures for ray tracing when source and receiver positions are known are given by Chander (1977); they are applicable to the situation of dipping planar layers. Because these methods yield frequency-independent results, the interference of waves arriving at the same time is found by determining the phase change along each ray path and summing the results.

Limitations on the usefulness of geometrical ray theory result from approximations that restrict its validity to situations in which changes in velocity or curvature are small over a wavelength, and from its inability to predict the following frequency-dependent effects: the arrival of body waves in shadow zones due to diffraction, the arrival of waves near a caustic (the envelope

where E = the amount of energy per unit time per unit solid angle emitted by a point source at the origin of the coordinate system
θ_0 = the angle with respect to the z-axis at which the ray leaves the source
x = the x-component of the distance along the ray path.

The decrease in intensity due to geometrical (cylindrical) spreading is $1/x$; the change in intensity due to changes in the cross-sectional area of the ray bundle caused by focusing is $\tan\theta_0/(\partial x/\partial\theta_0)$ (Officer 1974, p. 214). The assumption that energy does not cross rays implies that energy is neither diffracted according to wave theory nor scattered by inhomogeneities along the ray. The presence of wave energy in shadow zones, locations for which ray theory predicts no surface arrivals, is attributed to scatterers and the occurrence of diffraction that direct energy into the shadow zone (Urick 1983).

A ray in a homogeneous medium is traced using Snell's law,

$$\sin\theta_0/C = p$$

where p = constant for a given ray and is called the ray parameter
θ_0 = the angle the ray makes with the vertical to the surface (takeoff angle)
C = the wave velocity in the medium.

If wave velocity changes along the ray, the angle θ at which the ray is directed must change in order for p to remain constant. This relationship is given as

$$\frac{\sin\theta_0}{C_0} = \frac{\sin\theta_n}{C_n} = p \tag{5}$$

for an inhomogeneous medium modeled as n layers of constant velocity C_n; θ_n is the angle indicating the orientation of the ray in a layer of velocity C_n. As the thickness of the layers goes to zero, C is a continuous function of depth, $C(Z)$, and eq 5 can be written as

$$\frac{\sin\theta_0}{C(Z_0)} = \frac{\sin\theta}{C(Z)} = p$$

(Clay and Medwin 1977, p. 83; Telford et al. 1976).

There is additional information on the propagation of energy that can be obtained from ray theory (Officer 1974, Clay and Medwin 1977). The relationship between curvature of the ray, $d\theta/dS$, and velocity gradient, dC/dZ, is

$$\frac{d\theta}{dS} = p\frac{dC}{dZ}$$

where S is the coordinate distance measured along the ray. The ray is a straight line in a medium of constant velocity; it is a portion of a circle in a medium with a linear velocity profile, in which case the ray curves toward the region of minimum velocity. The ray becomes horizontal at a depth Z_p if

$$\sin\theta_0 = \frac{C(Z_0)}{C(Z_p)}$$

Solutions of the eikonal equation have the form $W(x, y, z)$ is constant and represent wave fronts. At a given time t, all points along a particular wavefront W will be in phase. A normal to the wave front along a particular wave front defines the direction of propagation and is a ray. Officer (1974) shows that

$$U = A(x, y, z)\, e^{i\omega [W(x,y,z)/C_0 - t]}$$

is a solution to the wave equation if the following equalities are true:

$$\left(\frac{\partial W}{\partial x}\right)^2 + \left(\frac{\partial W}{\partial y}\right)^2 + \left(\frac{\partial W}{\partial z}\right)^2 - n^2 - \frac{\lambda_0^2}{4\pi^2}\left[\frac{1}{A}\left(\frac{\partial^2 A}{\partial x^2} + \frac{\partial^2 A}{\partial y^2} + \frac{\partial^2 A}{\partial z^2}\right)\right] = 0$$

$$\frac{\partial^2 W}{\partial x^2} + \frac{\partial^2 W}{\partial y^2} + \frac{\partial^2 W}{\partial z^2} + \frac{2}{A}\left(\frac{\partial W}{\partial x}\frac{\partial A}{\partial x} + \frac{\partial W}{\partial y}\frac{\partial A}{\partial y} + \frac{\partial I}{\partial z}\frac{\partial A}{\partial z}\right) = 0 .$$

If

$$\frac{\lambda_0^2}{4\pi^2}\left[\frac{1}{A}\left(\frac{\partial^2 A}{\partial x^2} + \frac{\partial^2 A}{\partial y^2} + \frac{\partial^2 A}{\partial z^2}\right)\right] = 0$$

then W is a solution to the eikonal equation; here, $\lambda_0 = 2\pi C_0/\omega$ is the wavelength of the disturbance at angular frequency ω in the reference medium of velocity C_0. This condition is satisfied in the limit of high frequencies ($\lambda \to 0$). Of practical interest, W is a solution to the eikonal equation and U is a good approximation to a solution of the wave equation if $\lambda_0^2 (A''/A) \ll (W')^2$ (prime denotes differentiation with respect to a spatial coordinate). This condition can be rewritten to show that a solution to the eikonal equation will satisfactorily approximate a solution to the wave equation if 1) the fractional change in velocity gradient, $\delta C'$, over a wavelength is small compared with the gradient C/λ_0, ($\lambda_0 (\delta C'/C) \ll 1$), 2) the change of curvature of the wave front is small over a wavelength, ($\lambda_0 \delta W'' \ll 1$), or 3) the fractional change in the space rate of change of amplitude is small over a wavelength ($\lambda_0 (\delta A'/A) \ll 1$) (Officer 1974, p. 205).

The direction in which wave energy propagates is parallel to the rays. Because it is assumed that energy does not cross rays (i.e. the energy contained within a bundle of rays [raytube] at the source remains within the space defined by those rays) the propagation of energy through a medium becomes known by determining the paths of rays through the medium (Fig. 6). The space defined by a given bundle of rays changes due to geometrical spreading and due to changes in velocity with depth that result in focusing or defocusing of the rays. Accordingly, the intensity of the disturbance varies along the ray paths. The intensity at a point along a ray path between source and receiver at the same depth is given by

$$I(x, \theta_0) = \frac{E \tan\theta_0}{x(\partial x/\partial\theta_0)}$$

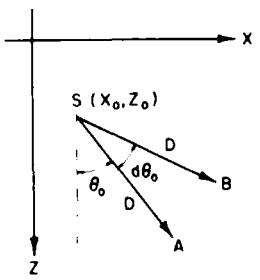

Figure 6. Rays A *and* B *emanating from a source* S *at takeoff angles of* θ_0 *and* $\theta_0 + d\theta_0$, *respectively. The rays are linear in a medium of constant velocity,* V. *In time* Δt, *each ray travels a distance* $D = V\Delta t$. *The location of ray* A *and the wave energy associated with it is then* ($X_0 + D \sin\theta_0$, $Z_0 + D \cos\theta_0$).

When the angle of incidence of a wave at an interface is real, the coefficients (transmission, reflection) for plane waves at planar interfaces are real and independent of frequency. The latter property means that there is no change in wave shape at the interface; i.e. the departing transmitted and reflected waves have the same shape as the incident wave but probably different amplitudes. If either the incident wave or the interface is nonplanar, there may be a change in pulse shape (a phase change) at the interface (Aki and Richards 1980, p. 155).

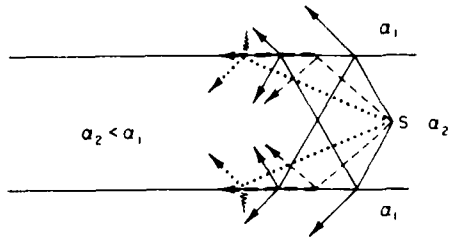

Figure 5. Reflected waves and transmitted waves generated by plane waves incident at the waveguide boundaries. At angles less than critical these are represented by solid rays. Reflected waves and head waves generated by plane waves that are critically incident at the waveguide boundaries are represented by dashed rays. Reflected waves generated by plane waves incident at angles greater than critical are represented by dotted rays; the associated inhomogeneous waves are represented by wavy lines.

The angle at which plane waves are incident at a boundary is crucial to the long-range propagation of wave energy within a layer or a waveguide (Fig. 5). When the angle of incidence is less than the relevant critical angle, wave energy is lost across each boundary in the form of transmitted (P, S) waves. When the waves are incident at the critical angle, reflected waves and a head wave exist and the wave energy is effectively trapped by the boundaries of the waveguide. When the angle of incidence is greater than the critical angle, the criterion for total reflection is satisfied but some energy is lost across the boundary from the inhomogeneous waves. The loss of energy from the waveguide is significantly lower when waves are incident at the waveguide boundaries at angles greater than critical.

The wave energy in a layer or waveguide may be described by a sum of normal modes. Each normal mode represents horizontally propagating waves that have the profile of standing waves in the z-direction; it is a solution to the wave equation and satisfies the boundary conditions of the problem. The stress-depth profile of a normal mode may be determined from an analysis of the constructive interference of plane waves that are totally reflected within the waveguide.

SECTION 3. BODY WAVES: RAY THEORY AND WAVE THEORY

Ray theory and wave theory are each the basis of analytical approaches to the study of the propagation of body waves in the earth. Their similarity is that each yields asymptotic solutions to the wave equation; their differences lie in the approximations used in their development and, consequently, in the restrictions on their validity.

Geometric ray theory

The concept of rays arises from the eikonal equation,

$$\left(\frac{\partial W}{\partial x}\right)^2 + \left(\frac{\partial W}{\partial y}\right)^2 + \left(\frac{\partial W}{\partial z}\right)^2 = \frac{C_0^2}{C^2} = n^2 , \qquad (4)$$

where C = velocity
C_0 = a constant, reference velocity
n = the index of refraction ($C_0/C \equiv n$).

where k_0 is an arbitrary constant used to define the wave number $k^2 = n^2 k_0^2$, n being the index of refraction. If f is assumed to vary slowly with respect to range, then $|\partial^2 f/\partial r^2| << |2k_0 (\partial f/\partial r)|$ and the Helmoltz equation is simplified to the parabolic wave equation $(\partial^2 f/\partial z^2) + 2ik_0(\partial f/\partial r) + (k^2 - k_0^2)f = 0$. Computer codes that solve the parabolic equation also are used in studying problems in underwater acoustics. The solution to the Helmholtz or the parabolic equation for particular boundary conditions (sound speed profile, source depth, receiver depth) is presented as a plot of propagation loss as a function of range for a specified frequency. Coppens (1982) discusses the use of the parabolic equation and cites errors in the calculated acoustic field that result from the assumption invoked in deriving it. One error is that the phase velocity of a particular normal mode obtained by solving the Helmholtz equation is different from the equivalent term obtained by solving the parabolic equation, and so the spatial pattern of the phase-coherent combination of the pressure terms will be different for the two solutions. The parabolic equation may be used under the conditions that the fractional change in velocity over one wavelength is small, and the angle of propagation with respect to the horizontal is small (Urick 1979).

When an integration over wave number is done to obtain an integral solution to the wave equation, a contour of integration along the real k-axis encounters no poles due to normal modes if the medium is assumed to be lossy. The Fast Field Program (FFP) uses the Fast Fourier Transform to numerically integrate the solution to the wave equation for the situation of lossy layers over a half-space and then removes the effect of attenuation due to anelasticity. The result is values of pressure, particle displacement, or velocity at range points $r_n = r_0 + n\Delta r$, $n = 0, 1, ..., N-1$. Which modes are included in the solution (normal, leaky) is determined by the range of wave numbers $k_m = k_0 + m\Delta k$, $m = 0, 1, ..., N-1$ selected. Kutschale (1973) notes that use of the FFP is quicker than use of normal mode theory in obtaining a solution to the wave equation because FFP solves the integral solution to the wave equation directly while normal mode theory requires that the roots of the dispersion equation be determined and then the corresponding normal modes be summed. Kutschale uses the FFP method to investigate how several factors (presence of a surface ice layer, rigidity of bottom sediments, source depth, small changes in sound speed profile in upper 400 m of water, variations in ice roughness) affect compressional wave propagation in the ocean.

SECTION 6. FINITE-DIFFERENCE METHOD

The basis of the finite-difference method is that it provides an exact solution to an approximation of a differential equation. In seismology it is the wave equation that is approximated. Whereas an analytic method provides a continuous solution to the wave equation, $u = u(x, z, t)$, a numerical method provides a discrete solution, $u = u(m\Delta x, n\Delta z, p\Delta t)$, to an approximation of the wave equation. The domain of the finite-difference solution is shown schematically in Figure 12 as a distribution of points in which the spacing between adjacent points is Δx parallel to the x-axis, Δz parallel to the z-axis, and Δt parallel to the t-axis. An introduction to the finite-difference method and its applications is given in many texts (e.g. Richtmeyer and Morton 1967, Lapidus and Pinder 1982).

Boore (1972) has reviewed the use of the finite-difference method in the study of seismic wave propagation. He cites the advantages of using this method as being the nature of the computations (a program to use the finite-difference method is easily written, is adapted readily to a variety of problems, and uses input data that are easily prepared) and the use of transient signals (because of which one computer run yields information on many frequencies). He also cites advantages in the presentation of results: displacement at a given position as a function of time (i.e the time series recorded by a seismometer), or displacement at a given time as a function of position (i.e. the total wave field). The finite-difference method is useful in solving problems for which there is no analytical solution or for which the analytical solution is more costly or less adaptable due to the com-

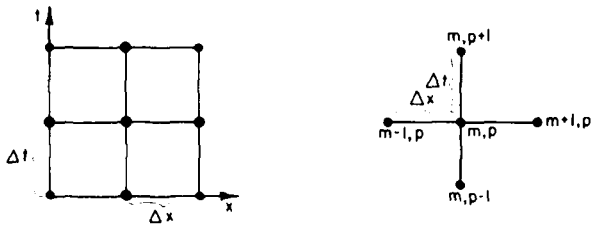

a. Finite-difference scheme for problems of one-dimensional wave propagation.

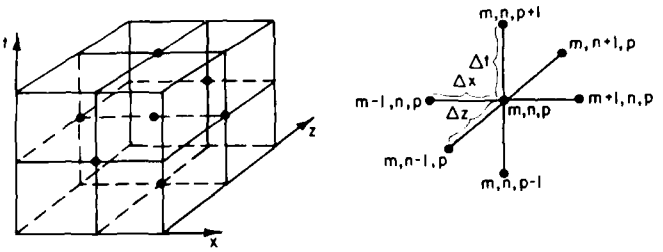

b. Finite-difference scheme for problems of two-dimensional wave propagation.

Figure 12. Grids and templates for finite-difference method. (adapted from Lapidus and Pinder 1982).

plexity of the physical model. Use of the finite-difference method is particularly advantageous with problems that concentrate on the near-field region of sources or that involve wave propagation through layered media in the case where the thickness of the layers is on the order of the seismic wavelengths. Another discussion of the finite-difference method as applied to seismology that includes more recent references is given by Aki and Richards (1980). Examples of the ways in which the numerical solution to the wave equation may be displayed are given in Figure 13.

There are two types of finite-difference schemes, both of which are recursive. To solve for the future displacement at a specified position, the explicit approach uses supplied or previously calculated values of displacement at that position and neighboring positions for past and present times. The implicit approach again uses known displacements at the specified position and neighboring positions, but for past, present and future times. In the notation used here, the explicit approach uses displacements at time levels $(p-1)$ and (p) to calculate displacements at time level $(p+1)$, while the implicit approach uses displacements at time levels $(p-1)$, (p), and $(p+1)$ to calculate displacements at time level $(p+1)$ (See Fig. 12). Emerman et al. (1982) investigated the use of an implicit finite-difference approximation of the wave equation and found it to be less accurate than the explicit formulation for the same size increments of space and time. Braile et al. (1983), however, compared four implicit formulations (including that of Emerman et al.) of the scalar wave equation with the explicit formulation of Alford et al. (1974); their results indicate that one of the implicit formulations provides reasonable accuracy with a grid spacing that is approximately twice as coarse (4 to 5 grid points per wavelength) as that required by the explicit and other implicit formulations, and thus results in a factor of four savings in computer storage and a factor of eight savings in computer time.

An understanding of the rather complex finite-difference equations given below can be gained by following the derivation of finite difference equations in the much simpler one-dimensional

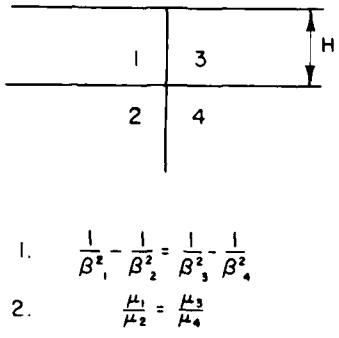

1. $\frac{1}{\beta_1^2} - \frac{1}{\beta_2^2} = \frac{1}{\beta_3^2} - \frac{1}{\beta_4^2}$

2. $\frac{\mu_1}{\mu_2} = \frac{\mu_3}{\mu_4}$

a. Geometry and media labels for four materials joining along a vertical interface. If the two conditions at the bottom are satisfied, an analytic solution to the problem of an incident Love wave can be found.

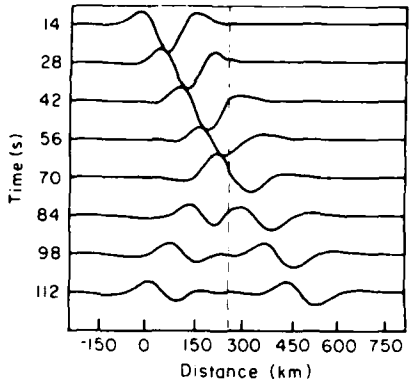

b. Surface displacements at different instants of time for the problem indicated in a. *The location of the vertical interface is given by the dashed line. The various elastic and geometric parameters, $\beta_1 = 3.85$, $\rho_1 = 3.0$, $\beta_2 = 4.75$, $\rho_2 = 3.65$, $\beta_3 = 4.23$, $\rho_3 = 7.44$, $\beta_4 = 5.53$, $\rho_4 = 8.07$, H = 35.0, were chosen such that a large reflected wave would be present. The units of β and ρ are km/s and g/cm^3.*

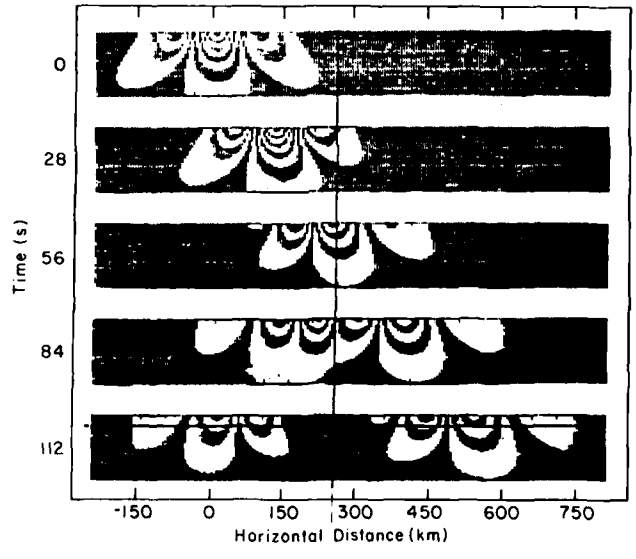

c. Computer-generated contour plots of the spatial distribution of Love-wave displacements at different instants of time for the problem illustrated in a. *The results here are derived from the same experiment as those in* b. *The top edge of each plot corresponds to the free surface. The vertical line denotes the vertical interface. The horizontal interface is shown in plot for T = 112. Vertical variation is distorted due to variable grid spacing with depth. Each plot can be viewed as a contour map of the displacements at each grid point for a certain instant of time, in which the area between every other contour is indicated by a given symbol.*

Figure 13. Application of the finite-difference method (from Boore 1970).

case. The x-axis is divided into segments of length ΔX that are bounded by grid points. The grid points are specified by $m\Delta X$, where $m = 0, 1, 2, \ldots$, and displacement at grid points is given by $U(m\Delta X) \equiv U_m$.

Finite-difference approximations to the partial derivatives $\partial U/\partial X = U_x$, $\partial^2 U/\partial X^2 = U_{xx}$ are obtained from a series expansion of $U(X)$. Two Taylor series for $U(X)$ about the point $(m\Delta X) \equiv X_m$ are

$$U(X_m + \Delta X) = U(X_m) + \Delta X\, U_x\big|_m + \frac{(\Delta X)^2}{2!}\, U_{xx}\big|_m + \frac{(\Delta X)^3}{3!}\, U_{xxx}\big|_m + \ldots \tag{14}$$

$$U(X_m - \Delta X) = U(X_m) - \Delta X\, U_x\big|_m + \frac{(\Delta X)^2}{2!}\, U_{xx}\big|_m - \frac{(\Delta X)^3}{3!}\, U_{xxx}\big|_m + \ldots \tag{15}$$

Equations 14 and 15 are solved individually for $U_x\big|_m$ to obtain

$$U_x\big|_m = \frac{U(X_m + \Delta X) - U(X_m)}{\Delta X} - \frac{\Delta X}{2!}\, U_{xx}\big|_m - \frac{(\Delta X)^2}{3!}\, U_{xxx}\big|_m - \ldots \tag{16}$$

$$U_x\big|_m = \frac{U(X_m) - U(X_m - \Delta X)}{\Delta X} + \frac{\Delta X}{2!}\, U_{xx}\big|_m - \frac{(\Delta X)^2}{3!}\, U_{xxx}\big|_m + \ldots \tag{17}$$

Two approximations to U_x at X_m are obtained from eq 16 and 17 by omitting terms in which ΔX is of the order 1 or higher:

$$U_x\big|_m \approx \frac{U(X_m + \Delta X) - U(X_m)}{\Delta x} \equiv \frac{U_{m+1} - U_m}{\Delta X} \tag{18}$$

$$U_x\big|_m \approx \frac{U(X_m) - U(X_m - \Delta X)}{\Delta X} \equiv \frac{U_m - U_{m-1}}{\Delta X}\,. \tag{19}$$

Equation 18 is termed a forward difference; $U_x\big|_m$ is determined by the displacements at X_m and the adjacent, higher index grid point, X_{m+1}. Equation 19 is termed a backward difference; $U_x\big|_m$ is determined by the displacements at X_m and the adjacent, lower index grid point, X_{m-1}.

A central difference approximation to $U_x\big|_m$ is obtained by adding eq 16 and 17 and solving for $U_x\big|_m$:

$$U_x\big|_m = \frac{U_{m+1} - U_{m-1}}{2\Delta X}\,. \tag{20}$$

By subtracting eq 17 from eq 16 and solving for $U_{xx}\big|_m$, the following finite-difference approximation to $\partial^2 U/\partial X^2$ is obtained:

$$U_{xx}\big|_m = \frac{U_{m+1} - 2U_m + U_{m-1}}{(\Delta X)^2}\,.$$

The first term of the series remainder is $-((\Delta X)^2/12)\, U_{xxxx}\big|_\epsilon$ where $X_m - \Delta X \leqslant \epsilon \leqslant X_m + \Delta X$.

The equation which Boore (1972) used in his study of Love surface waves and *SH* body waves is

$$u^{p+1}_{m,n} = 2u^p_{m,n} - u^{p-1}_{m,n} + \beta^2\,(\Delta t)^2\, \frac{u^p_{m+1,n} - 2u^p_{m,n} + u^p_{m-1,n}}{(\Delta x)^2} + \frac{u^p_{m,n+1} - 2u^p_{m,n} + u^p_{m,n-1}}{(\Delta z)^2}$$

where $u^{p}_{m,n}$ is notation for displacement at a point $(m\Delta x, n\Delta z)$ at a time $p\Delta t$ and $\beta^2 = (\mu/\rho)^2$. This equation is a finite-difference approximation to the partial differential equation for displacement in the y-direction in a homogeneous medium, $\partial^2 u/\partial t^2 = \beta^2(\partial^2 u/\partial x^2 + \partial^2 u/\partial z^2)$. It is correct to second order in the increments. In the case of an inhomogeneous medium,

$$u^{p+1}_{m,n} = 2u^{p}_{m,n} - u^{p-1}_{m,n}$$

$$+ \frac{(\Delta t)^2}{\rho_{m,n}} \left[\frac{\mu_{m+\frac{1}{2},n} u_{m+1,n} - (\mu_{m+\frac{1}{2},n} + \mu_{m-\frac{1}{2},n})\, u_{m,n} + \mu_{m-\frac{1}{2},n} u_{m-1,n}}{(\Delta x)^2}\right]$$

$$+ \frac{(\Delta t)^2}{\rho_{m,n}} \left[\frac{\mu_{m,n+\frac{1}{2}} u_{m,n+1} - (\mu_{m,n+\frac{1}{2}} + \mu_{m,n-\frac{1}{2}})\, u_{m,n} + \mu_{m,n-\frac{1}{2}} u_{m,n-1}}{(\Delta z)^2}\right]$$

(Aki and Richards 1980, p. 781).

The wave equation for the situation of in-plane waves (*P-SV*, Rayleigh) propagating in a homogeneous isotropic body is

$$\frac{\partial^2 u}{\partial t^2} = \alpha^2 \frac{\partial^2 u}{\partial x^2} + (\alpha^2 - \beta^2) \frac{\partial^2 w}{\partial w \partial z} + \beta^2 \frac{\partial^2 u}{\partial z^2}$$

$$\frac{\partial^2 w}{\partial t^2} = \alpha^2 \frac{\partial^2 w}{\partial z^2} + (\alpha^2 - \beta^2) \frac{\partial^2 u}{\partial x \partial z} + \beta^2 \frac{\partial^2 w}{\partial z^2}$$

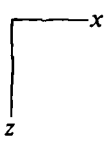

In vector form the wave equation is

$$\frac{\partial^2 \mathbf{u}}{\partial t^2} = \mathbf{A}\frac{\partial^2 \mathbf{u}}{\partial x^2} + \mathbf{B}\frac{\partial^2 \mathbf{u}}{\partial x \partial z} + \mathbf{C}\frac{\partial^2 \mathbf{u}}{\partial z^2}$$

where $\mathbf{u} = \begin{pmatrix} u \\ w \end{pmatrix}$

$$\mathbf{A} = \begin{pmatrix} \alpha^2 & 0 \\ 0 & \beta^2 \end{pmatrix}$$

$$\mathbf{B} = \begin{pmatrix} 0 & \alpha^2 - \beta^2 \\ \alpha^2 - \beta^2 & 0 \end{pmatrix}$$

$$\mathbf{C} = \begin{pmatrix} \beta^2 & 0 \\ 0 & \alpha^2 \end{pmatrix}.$$

Aki and Richards (1980) (citing Alterman and Rotenburg 1969) give the following finite-difference approximation to the wave equation:

$$\mathbf{u}(x, z, t + \Delta t) = 2\mathbf{u}(x, z, t) - \mathbf{u}(x, z, t - \Delta t) + \mathbf{A}\left(\frac{\Delta t}{\Delta x}\right)^2 [\mathbf{u}(x + \Delta x), z, t) - 2\mathbf{u}(x, z, t)$$

$$+ \mathbf{u}(x - \Delta x, z, t)] + \mathbf{B}\frac{(\Delta t)^2}{4\Delta x \Delta z} [\mathbf{u}(x+\Delta x, z+\Delta z, t) - \mathbf{u}(x+\Delta x, z-\Delta z, t)$$

$$- \mathbf{u}(x-\Delta x, z+\Delta z, t) + \mathbf{u}(x-\Delta x, z-\Delta z, t)] + \mathbf{C}\left(\frac{\Delta t}{\Delta z}\right)^2 [\mathbf{u}(x, z+\Delta z, t) -$$

$$- 2u(x, z, t) + u(x, z - \Delta z, t)] .$$

This finite-difference equation is correct to second order in the increments. Aki and Richards also give Alterman and Karal's (1968) finite-difference equation for spherical waves propagating from an explosive source in a layered medium, and a finite difference equation for one-dimensional wave propagation in the case where wide-angle scattering, back-scattering, and reflection are negligible; the latter equation is suited to the study of wave propagation in a laterally varying medium from a teleseismic source.

The wave equation (constitutive equation) can be approximated by several different finite difference equations that may all approach the differential equation in the limit that Δx (and Δz) and Δt approach zero, but that may have different solutions when the increments are finite. In general, the choice of a finite difference equation to approximate a differential equation affects the accuracy and stability of the numerical solution. Equations 18, 19 and 20 are all finite-difference approximations to $U_x|_m$. A measure of the error that results from the finite-difference approximation is given by the first term of the truncated series expansion of $U(X)$:

$$\pm \frac{\Delta X}{2} U_{xx}|_\epsilon \begin{cases} X_m \leqslant \epsilon \leqslant X_m + \Delta X \text{ (eq 16)} \\ X_m - \Delta X \leqslant \epsilon \leqslant X_m \text{ (eq 17)} \end{cases}$$

$$- \frac{(\Delta X)^2}{6} U_{xxx}|_\epsilon, \; X_m - \Delta X \leqslant \epsilon \; X_m + \Delta X \text{ (eq 20)}$$

Lapidus and Pinder (1982) list finite-difference approximations to derivitives for the cases of one and two dependent variables, and list the order of error resulting from truncation of the series. Aki and Richards (1980) evaluate the stability (i.e. does the error due to approximating derivitives grow as the numerical solution proceeds, or does it remain bounded?) of various finite difference schemes for wave propagation *in one* direction, as given by

$$\frac{\partial \dot{u}}{\partial t} = \frac{1}{\rho(x)} \frac{\partial \Gamma}{\partial x}$$

where $\dot{u} = \partial u/\partial t$
$\Gamma = E(x)\, \partial u/\partial x$
$E(x) = \lambda(x) + 2\mu(x)$, P-waves
$E(x) = \mu(x)$, S-waves.

They find that a scheme using a central difference for the x-derivitive and a forward difference for the t-derivitive is unstable, while a scheme using central differences for both derivitives is stable if restrictions on Δt and Δx are met. The optimum scheme that Aki and Richards consider involves staggered grids, with the grid for $\dot{u}$ being displaced from the grid for Γ by half a grid spacing in both x and t; the use of central-difference approximations leads to an error equal to ¼ of the error of the latter scheme above (because the error is proportional to the square of the sampling interval) while having the same stability criterion.

A criterion for stability has the form $\Delta t \leqslant \Delta x/c$, where c is the local wave velocity. For a solution to be stable, the time interval between adjacent grid points must be less than or equal to the time required for a wave to propagate over the space interval between adjacent grid points. When this criterion is met, $u(m+1, n)$ is uniquely determined by $u(m, n-1)$, $u(m,n+1)$ and $u(m-1, n)$. The stability condition for SH-wave or Love wave propagation in a uniform medium of n space dimensions is $\beta\Delta t/\Delta x \leqslant 1/\sqrt{n}$ (Boore 1972). The stability criterion for the two-dimension in-plane (P-SV and Rayleigh) wave problem described above is $\Delta t/\Delta x \leqslant 1/(\alpha^2 + \beta^2)^{½}$ (Aki and Richards 1980, p. 782).

Since the finite-difference method results in a solution to the constitutive (wave) equation only at net points, it would seem logical to use a net of small grid size so that the problem is well resolved spatially and temporally. The cost to obtain the numerical solution, however, is dependent primarily on the number of calculations that must be performed and on the storage space required, and so is ultimately determined by the grid spacing. A compromise approach is to use a fine grid size early in the numerical solution, such as near a seismic source, and then to rezone the grid to a larger spacing as the problem progresses, i.e. at net points corresponding to later times and distant positions (Cooper 1971). A difficulty of the rezoning technique is that intensive (mass independent) quantities such as pressure or velocity that are initially specified for the case of the individual, small grid zones must now be appropriately determined for the larger, composite zone. In a study of Love-wave propagation in a plane-layered medium, Boore (1972) increased the grid spacing with depth in order to delay the arrival of waves reflected from the boundary of the region of interest; this modification, based on the decay with depth of Love wave arrivals, has had mixed success. The maximum storage space required by an explicit finite difference scheme is $2(NX)(NZ)$, where NX and NZ are the number of grid points in the x and z directions (Boore 1972). Although each time level requires $(NX)(NZ)$ storage spaces and although displacements at two time levels (p, p-1) are needed to calculate the displacements at the next time level (p+1), once $u^{p+1}_{m,n}$ is calculated $u^{p-1}_{m,n}$ is no longer needed so storage locations for the (p-1) data may be used for the (p+1) data.

Application of the finite difference method to determine future displacement requires that either the displacement at each net point be known at times $t = 0$ and $t = \Delta t$, or that velocity and displacement at time $t = 0$ be known. In studying wave propagation in an inhomogeneous medium, it is customary to situate the seismic source in an adjacent laterally homogeneous medium so that displacement at $t = 0$, Δt (or displacement and particle velocity at $t = 0$) can be determined from an analytic solution. Displacement is zero throughout the inhomogeneous region until sufficient time has passed (determined by distance from source and velocity of homogeneous region) for the disturbance to arrive at the boundary between the two regions; changes in displacement with time are then determined numerically as the disturbance propagates through the inhomogeneous region. The theoretical displacements at times $t = 0$ and $t = \Delta t$ that are consistent with a given surface wave shape are synthesized using a Fast Fourier Transform method (Boore 1970, Fuyuki and Matsumoto 1980).

Wave propagation problems studied by seismologists customarily involve physical boundaries such as a free surface, interfaces of layered media or the perimeter an inhomogeneous region. Alterman and Loewenthal (1972) describe a technique for using finite-difference equations for boundary conditions in order to obtain displacements at a free surface or at an interface. In both situations the finite difference net is extended past the physical boundary (free surface, interface) so that the boundary no longer terminates the net superimposed on the half-space or layer. Displacements at net points on the fictitious line (the extension of the net) are used in the finite difference equations of motion to calculate displacements up to and including the physical boundary. This approach is used also by Kelly et al. (1976) and Fuyuki and Matsumoto (1980).

Additional boundaries are introduced when the finite difference method is used in order to restrict the size of the domain for which the numerical solution is obtained in accordance with the amount of computer storage available. These artificial boundaries are sources of reflected waves, which will affect the numerical solution adversely only when sufficient time has passed for the reflected waves to have propagated into the region of interest. Boore (1972) recommends that numerical experiments using different distances to the imposed boundaries be done in order to define the space-time region that is free of contamination by waves introduced by the presence of artificial boundaries. The artificial boundaries can be characterized so that wave energy is absorbed (Fuyuki and Matsumoto 1980) or reflections are canceled due to the superposition of solutions of opposite sign (Smith 1974).

Complications with a numerical solution that arise due to the use of a discrete grid are aliasing (false representation of frequency content) of the continuous time series and dispersion of waves propagating on a lattice. These complications can be avoided by restricting the frequency-dependent information that is extracted from the numerical solution (Boore 1972). The problem of aliasing can be alleviated by regulation of the source so that little or no power is present at values of wave number above the Nyquist wave number, which is inversely proportional to grid spacing. The effects of lattice-induced dispersion can be eliminated by ignoring information at wavelengths for which there are 10 or fewer net points per wavelength. Alford et al. (1974) showed that, with an explicit second-order difference scheme, there is little dependence of phase velocity and group velocity on stability ratio ($c\Delta t/\Delta x$) for $\Delta x/\lambda < 0.1$, where λ is wavelength, at the upper half-power frequency of the source.

Table 1 lists examples of problems for which synthetic seismograms were generated using the finite-difference method.

Table 1. Applications of the finite-difference method to seismology.

Problems studied with finite-difference method	*Wave type/source*	*Reference*
Lateral heterogeneity: uniform layer of nonconstant thickness (w/planar free surface) covering a homogeneous half-space	Love wave	Boore (1970, 1972)
Pair of layers over quarter-space with vertical interface	Love wave	Boore (1970, 1972)
Sloping layer	Love wave	Boore (1970, 1972)
Sloping interface: 1) crust/mantle interface 2) basin	*SH*-waves at vertical incidence	Boore et al. (1971), Boore (1972)
Semi-infinite medium with surface topography	*SH*-waves at vertical incidence	Boore (1972)
90° wedge (quarter-space) in otherwise infinite homogeneous medium	Line source tangent to apex of wedge. Includes case of diffracted waves	Alford et al. (1974)
Problems of interest in exploration tion seismology: homogeneous layers separated by plane, horizontal interface, includes case of a weathered layer quarter-space embedded in a half-space fluid (brine, gas) saturated, 100-ft-thick sandstone layer embedded in shale Also heterogeneous case: elastic constants specified at each net point	Compressional (*P*-) wave line source located within upper layer Waves evident: direct *P*-waves surface reflected *P*-waves head waves *P*-waves converted into *S*-waves by reflection Rayleigh waves diffracted waves	Kelly et al. (1976)
Scattering at a trench	Rayleigh wave	Fuyuki and Matsumoto (1980)
Layered half-space: cylindrical coordinates	Pressure pulse	Alterman and Loewenthal (1972)
Impulsive line source located in interior of quarter-space or in interior of three-quarter-space	*P*-waves	

Table 1 (cont'd). Applications of the finite-difference method to seismology.

Problems studied with finite-difference method	*Wave type/source*	*Reference*
Heterogeneous medium: spherical coordinates	Impulsive point source	
Shearing stress acting on a crack in a plane (deep focus earthquake)		
Shearing stress acting on a crack in a half-plane (dip-slip on a vertical fault which breaks free surface)		
Impulsive line source located inside one of two welded quarter-spaces		
Dislocation source in a homogeneous half-space	*S*-waves, *P*-waves/ Dislocation source	Braile et al. (1983)
Dislocation source in a laterally heterogeneous velocity structure model; dislocation source is located on a subducting slab		
Layer over half-space	Love waves	Kelly (1983)
Thickening channel	Conversion to body waves evident	Note: data band-pass filtered to isolate frequency components so as to display modes
Thinning channel		
Irregular layer/half-space interface		
Channel with low velocity fill over subsided layer and subsided half-space		
Channel filled with same material as subsided layer		
Channel with high velocity fill over subsided layer and subsided half-space		
Layer over two quarter-spaces		
Layer over angular unconformity		
Periodic channels in upper portion of layer		

SECTION 7. FINITE-ELEMENT METHOD

There are a number of similarities between the finite-element and the finite-difference methods. Both involve the division of a continuous, two-dimensional structure into discrete portions defined by nodes (or net points), both yield numerical solutions whose accuracy is dependent on the spacing between nodes relative to wavelength, and both assume that the displacements of nodal points define the complete displacement field for the structure. The distinction between the methods is that the finite-difference solution is obtained at discrete points by approximating the differential equations that describe a problem involving an elastic continuum, while the finite-element solution is obtained by approximating the elastic continuum as a composite of structural elements whose internal displacements are known by interpolation. Information on the finite-element method is found in books on solving partial differential equations (e.g. Lapidus and Pinder 1982) and in examples of the application of the method, e.g. structural mechanics (Clough 1965) and propagation of seismic waves (Lysmer and Drake 1972, Smith 1975).

The finite element-method requires that a structure be divided into a finite number of plane elements that meet at nodes. The commonly used elements are quadrilaterals and triangles. The nodes need not be regularly spaced; the configuration of the elements can be such that the mesh closely fits an irregularly shaped structure. As with the finite-difference method, there is a trade-off between accuracy (determined by the number of elements, i.e. element size) and cost (determined by the amount of storage and the number of calculations required).

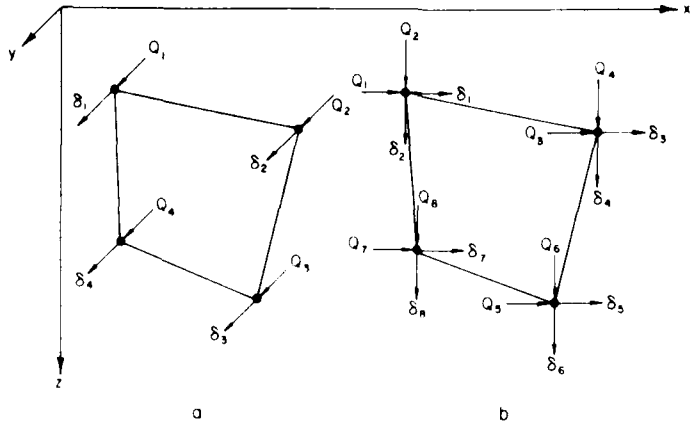

Figure 14. Forces Q *and displacements* δ *at nodes of a quadrilateral element are shown for the cases of a)* SH *or Love waves and b)* P *and* SV *or Rayleigh waves (from Lysmer and Drake 1972).*

An assumption inherent to the finite-element method is that all external forces and forces between elements are transmitted through nodal points. Each nodal point has one or two force components acting on it, depending on whether the wave motion considered is one-dimensional (*SH* waves, Love waves) or two dimensional (*P* and *SV* waves, Rayleigh waves), and has the same number of displacement components (Fig. 14a, b). Three requirements that must be satisfied simultaneously are those of equilibrium, compatibility, and force-deflection relationship, i.e. the internal element forces acting at each nodal point must equilibrate the externally applied nodal force, the deformations of the elements must be such that the elements continue to meet at the nodal points in the loaded condition, and the internal forces and internal displacements within each element must be related as required by its individual geometry and material properties (Clough 1965). Displacements of points within an element are defined by displacement functions in terms of the displacements at nodes. A linear element is one for which the internal displacements are linearly interpolated from the nodal displacements. Displacement functions are chosen so that the type of element is unchanged as a disturbance propagates through it (i.e. quadrilateral elements remain quadrilateral), which satisfies the displacement compatibility conditions on the boundaries between elements. The numerical solution is obtained either for the case of a forcing function or for the case of specified initial displacements and velocities.

Displacements of nodal points are related to forces through the stiffness matrix $[K]$. If the loading is static,

$$[K]\{\delta\} = \{Q\}. \tag{21}$$

Here $\{\delta\}$ is a column vector which represents the displacement field; the size of $\{\delta\}$ is determined by the number of nodal points (N) and by the degrees of freedom at each nodal point ($\{\delta\}$ is of size N in the case of Love or *SH* waves, $2N$ in the case of *P* and *SV* or Rayleigh waves). The column vector $\{Q\}$ represents the external forces applied to the structure; it is of the same size as $\{\delta\}$. Once $[K]$ is known, eq 21 is solved for the displacements $\{\delta\}$. If the loading is dynamic (time dependent), an inertia term must be included and

$$[M]\{\delta''\} + [K]\{\delta\} = \{Q\} \tag{22a}$$

(Lysmer and Drake 1972). If a damping matrix $[C]$ is included,

$$[M]\{\delta''\} + [C]\{\delta'\} + [K]\{\delta\} = \{Q\} \tag{22b}$$

(Smith 1975). Here $[M]$ is a mass matrix. The prime denotes differentiation with respect to time. Once $[M]$ and $[K]$ (and $[C]$, if included) have been determined, eq 22a, b may be solved for the displacements $\{\delta\}$. When the excitation of the structure is assumed to be harmonic, with angular frequency ω, steady-state problems can be solved by the method of complex response (Lysmer and Drake 1972). Assume that $\{P\}$ is a time-independent, complex force amplitude and $\{u\}$ is a time-independent, complex displacement amplitude. Let

$$\{Q\} = \{P\}\exp(i\omega t) \tag{23}$$

and

$$\{\delta\} = \{u\}\exp(i\omega t). \tag{24}$$

Substitution of eq 23 and 24 into 22b results in

$$([K] - \omega^2[M])\{u\} = \{P\} \tag{25a}$$

$$([K] + i\omega[C] - \omega^2[M])\{u\} = \{P\}, \tag{25b}$$

each of which is a set of linear equations to be solved for displacement amplitude $\{u\}$. This approach is correct for problems involving surface waves or for problems involving body waves when the wavelength is greater than the scale size. For body wave problems in which the scale size is greater than the wavelength, eq 22a, b must be solved in the time domain (Smith 1975). Lysmer and Drake (1972) describe how the matrices $[M]$ and $[K]$ are determined for the solution in the frequency domain. The procedure involves first determining the mass $[M']$ and stiffness $[K']$ matrices for each element and then assembling the element matrices to form $[M]$ and $[K]$. Because $[M']$ and $[K']$ are determined for a local coordinate system convenient for the configuration of the element, they must be transformed into a global coordinate system before being added to give $[M]$ and $[K]$. Smith (1975) uses the lumped mass matrix which is preferred for problems in the time domain.

As with any numerical procedure, the accuracy of the solution obtained with the finite-element method must be evaluated. Smith (1975) determined that for the case of a plane wave propagating a distance of 1 km through linear, rectangular elements, attenuation is negligible and dispersion is $\approx 1\%$ for a mesh size of 10 elements per wavelength; attenuation and dispersion are each 3% when there are 8 elements per wavelength. These results are dependent on the time-stepping algorithm and on the length of the time step Smith used. Eight to 12 elements and 6 to 10 elements per wavelength are also cited in the literature. Accuracy is also affected by the interpolation used to define displacements within an element. The spacing and configuration of the elements can be varied in accordance with the resolution needed in a particular portion of the finite element model. Contamination of the solution by waves reflected from artificial boundaries (sides and bottom of model) is avoided through the use of nonreflecting boundaries or by terminating the solution before the spurious waves reach the region of interest.

Geller et al. (1979) determined the dynamic finite-element solutions for displacements and velocities observed at the surface due to movement on a fault modeled as a dislocation. Their results are compared with the analytic solution in Figures 15a and 15b. The agreement between the analytic solution and the numerical solution is worse when the size of the elements is doubled because the resolution due to high frequency components is lost; there is an insufficient number of elements per wavelength at the high frequencies when the element size is increased. The agreement between the analytic and the numerical solutions is better for displacements than for veloc-

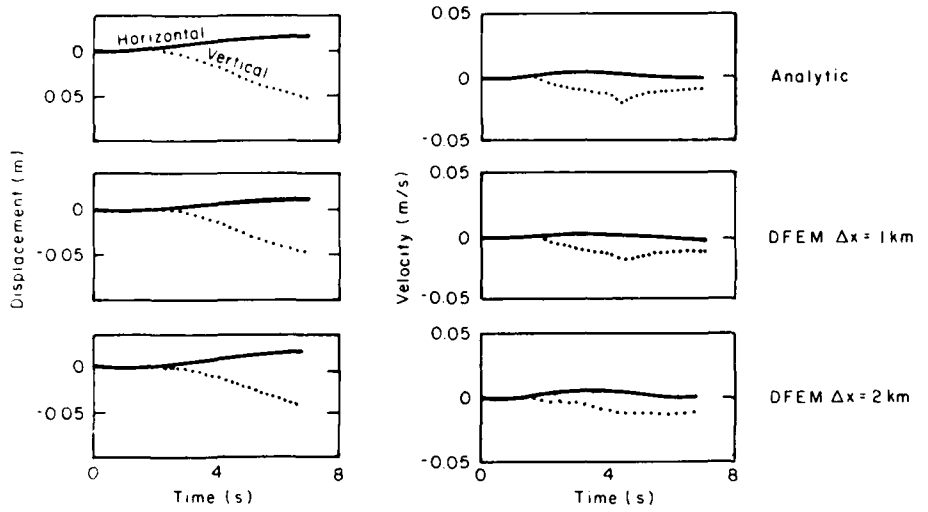

a. Displacement and velocity at a surface location 0.5 km above and 5 km off the fault.

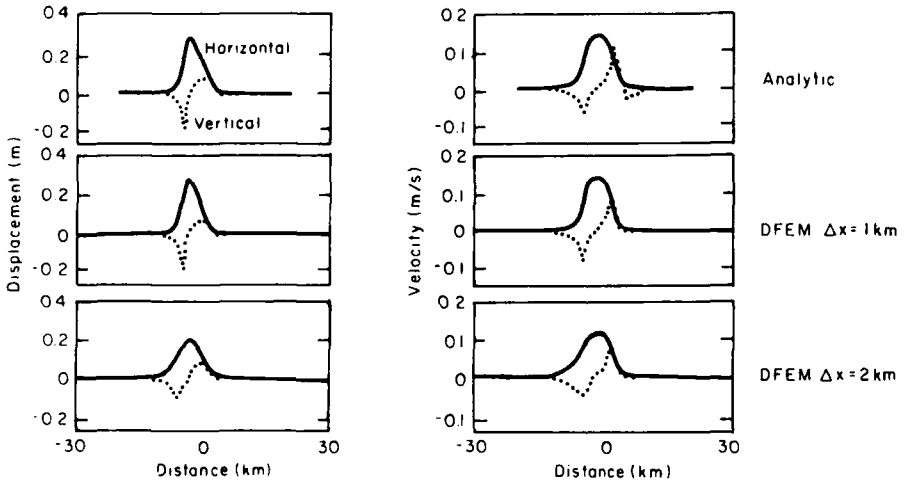

b. Displacement and velocity at the surface along the fault strike. The fault extends from **X** *= -5 km to* **X** *= 5 km at a depth of 0.5 km.*

Figure 15. Calculated values of ground motion due to movement along a right-lateral fault. Results are given for the analytic solution and for numerical solutions with different element sizes (from Geller et al. 1979).

ities because the displacements have a lower predominant frequency and are thus less affected by the use of a discrete representation.

Examples of problems involving wave propagation to which the finite element is well suited are given below.

Lysmer and Drake (1972) apply the finite element method to the study of the propagation of surface waves in a layered medium and in a region of irregular structure. They define a generalized Love wave to be any free motion involving harmonic displacements of the form $\delta = u(z) \exp i(\omega t - kx)$ in an infinite n-layered structure with horizontal interfaces. Here k is the wave number and $u(z)$ is the amplitude function. If the function $u(z)$ is assumed to vary linearly within each layer, then a discrete representation of the Love wave is

$$\{\delta\} = \alpha \{u\} \exp i(\omega t - kx),$$

where $\{\delta\}$ is a column vector containing the displacements $\delta_j, j = 1, 2, ..., n$ of the layer interfaces, $\{u\}$ is a complex amplitude vector with the components $u_j, j = 1, 2, ..., n$, and α is a mode participation factor which indicates the contribution of each mode to the amplitude of the displacement. The assumption of linear variation of the amplitude function is valid if the thicknesses of the model layers are small compared to the wavelengths of the shear waves in the layer; this requirement may necessitate introducing more layers than there are actual structural layers present in the model. The equation of free harmonic motion is

$$([A]k^2 + [G] - \omega^2 [M])\{u\} = \{0\},$$

where the matrices $[A]$ and $[G]$ are related to the stiffness of the layered structure. Boundary conditions are given for the case of an irregular zone between two semi-infinite layered zones. The irregular zone has surface topography and layers with sloping or nonplanar interfaces. Vertical interfaces separate the irregular zone from the semi-infinite layered regions. A restriction on the thickness of layers (relative to wavelength) within the semi-infinite zones was given above; an additional restriction is that the interfaces between those layers must coincide with nodal points on the vertical interfaces with the irregular zone. Lysmer and Drake (1972) give the results from two problems, propagation of Love waves across an idealized alluvial valley and propagation of Rayleigh waves through a portion of the Central Valley of California and the Sierra Nevada.

Smith (1975) gives the results of a finite-element study of three body wave propagation problems: the amplification of ground motion by surface topography (mountain), amplification of ground motion due to a semicylindrical alluvial valley, and ground motion due to a deep focus earthquake (case of a subducting slab).

Bolt and Smith (1976) use the finite-element method to compute synthetic seismograms for *P*-waves vertically incident on a massive sulfide ore body and for *SH*-waves vertically incident on a buried salt dome.

McCowan et al. (1977) use observed ground motions from the San Fernando, California (9 Feb 1971), earthquake as the displacements in two-dimensional finite-element model of the fault. They first consider the static case (eq 21) and solve the inverse problem for the force vector. They then use the same finite-element model for the dynamic case (eq 22b) and compute synthetic seismograms. Finite-difference equations are used to relate acceleration and velocity to displacement in the dynamic problem.

Melosh and Raefsky (1981) utilize the technique of split nodes in order to advantageously treat the presence of faults or cracks in a finite element model. In a standard finite-element scheme, elements that share a node experience the same displacement at that node; the distinguishing characteristic of a split node is that its displacement varies with the element under consideration. In this way, a split node located on a fault has two displacement values, the first (u^+) ex-

perienced by the element on one side of the fault, the second (u^-) experienced by the element on the opposite side of the fault. Melosh and Raefsky state that the use of split nodes does not compromise the accuracy or stability of the computation.

SECTION 8. HYBRID METHODS

The characteristics of a problem may determine that it is advantageous to employ a method of generating synthetic seismograms that is based upon ray theory rather than mode theory, or vice versa. Table 2 (from Urick 1983, p. 122) compares normal mode and ray theories. A normal mode approach handles initial conditions well and is useful at low frequencies (below 500–1000 Hz depending on the model used), while a method based upon ray theory handles boundary conditions well and is appropriate for programs involving high frequencies and long propagation distances; although mode theory is valid at all frequencies, its use at high frequencies effectively is restricted to short propagation distances. Hybrid methods that have features of both ray theory and normal mode theory may have lower computational cost yet retain sufficient accuracy. RAYMODE, a computer program written for underwater acoustics, is a hybrid method applicable to studies of compressional wave propagation at a range of frequencies (low to high) in a medium characterized by depth-dependent velocity and a flat lower boundary at which there may be loss of energy.

Another hybrid ray-mode formulation developed for studies of wave propagation in waveguides and ducts (Felsen and Ishihara 1979, Felsen 1981) has been used to construct synthetic seismograms for the case of *SH*-waves in a layer over a half-space (Kamel and Felsen 1981). This method employs a truncated ray series, each ray characterized by its takeoff angle at the source, and a truncated mode series, each mode characterized by the angle of incidence of its equivalent plane waves at the layer boundaries; together, the two series constitute a complete spectrum of angles while avoiding problems such as caustics by the appropriate selection of rays to be incorporated in the solution. Because the total number of generalized rays and normal modes contained in this hybrid formulation generally is less than the number of rays or of modes required when either method is employed independently, the computational cost of the hybrid method is lower. This hybrid method, developed for the case of high frequencies, includes asymptotic approximations and results in a solution of the wave equation comprised of generalized rays, normal modes, and a remainder; Felsen (1981) notes that if the asymptotic approximations are not used, the hybrid formulation is exact. Synthetic seismograms generated by four methods were compared. The hybrid formulation consisted of two generalized rays (direct and singly reflected), two trapped modes,

Table 2. Comparison of normal-mode and ray theories (from Urick 1983).

Normal-mode theory	*Ray theory*
Gives a formally complete solution.	Does not handle diffraction problems, e.g. sound in a shadow.
Solution is difficult to interpret.	Rays are easily drawn. Sound distribution is easily visualized.
Cannot easily handle real boundary conditions.	Real boundary conditions are inserted easily, e.g. a sloping bottom.
Source function easily inserted.	Is independent of the source.
Requires a computer program, except in limiting cases when analytic answers exist, and presents computational difficulties in all but simplest boundary conditions.	Rays can be drawn by hand using Snell's law. However, a ray-trace computer program is normally used.
Valid at all frequencies, but practically is useful for low frequencies (few modes).	Valid only at high frequencies if (1) radius of ray curvature is $> \lambda$ or (2) sound velocity does not change much in a λ, i.e. $(\Delta V/V)/\Delta z << 1/\lambda$.

and a remainder. The method of generalized rays (Cagniard-de Hoop) incorporated 14 rays. Seismograms generated by these two methods were indistinguishable. The seismogram obtained by a solution equivalent to the hybrid formulation without the remainder term agreed with that of the hybrid method for early observation times but became in error at a time corresponding to the arrival of the singly reflected ray; from then on, the discrepancy between the two seismograms decreased with time. The fourth seismogram, based upon the two trapped modes incorporated in the hybrid solution, was initially in error but approached agreement with that of the hybrid method with time.

A second type of hybrid method is one which combines analytical and numerical methods of solving the wave equation. Shtivelman (1984) uses the finite difference method and a form of asymptotic ray theory to compute the wave field in media having irregular structures. The finite difference method is used in the vicinity of a scatterer or complex structure because the numerical method generally handles wave propagation in heterogeneous media well, whereas the ray method is unsuitable when scattering from heterogeneities or wave propagation through thin beds is involved. The ray method is used to compute the wave field in homogeneous regions or in regions where layers are thick relative to wavelength because in such cases the computational cost and storage requirements of the finite difference method, together with the possibility of numeric dispersion causing loss of accuracy, cause it to be the less suitable method. The transition between methods occurs at an arbitrary contour along which the wave field of the first method employed is used to define source terms for the second method. Shtivelman gives examples of the application of this hybrid method to the case of *SH* plane waves impinging on an interface that is displaced by a right angle step, an inclined step, a right angle projection, a right angle recess, or a thrust fault.

SECTION 9. CONCLUSION

Several methods of generating synthetic seismograms have been reviewed. The selection of a method for use is based upon considerations of the physical aspects of a problem—complexity of the geologic model, wave types to be included in the seismogram—and of computational cost. The type of problem for which various methods are appropriate is indicated by Table 3, in which specific computer codes are evaluated by Braile (1982), and by Table 4.

Table 3. Summary of seismic interpretation techniques (from Braile 1982).

Method	*Characteristics*	*Limitations*
Travel-time Analysis		
Geometrical Ray theory calculation of travel-times of reflected and refracted phases (Program TXCURV).	Travel-times for head waves and reflections for plane or dipping layered models; exact.	Model geometry; travel-time only.
Ray Tracing (Program RAY2D).	Two-dimensional models.	Travel-times only; limited number of phases; ignores *P-S* conversions, guided waves and surface waves.
Synthetic Seismogram Modeling		
Reflectivity (Program SYNCAL).	Wave-theoretical solution to response of a layered half-space. Includes *P, SV,* guided phases and surface waves. Exact. Includes *Q.*	Restricted to 1-D models.

Table 3 (cont'd).

Method	*Characteristics*	*Limitations*
Disk Ray Theory (modified RAY2D program).	2-D models, approximate solution for *P* waves, can include reflection coefficients and *Q*. Computationally efficient.	Inexact amplitudes for head waves and near-critical arrivals; ignores guided phases, *P-S* conversions and surface waves.
Finite Difference Acoustic (Program FDWVAC)	2-D models, *exact* solution for *all* wave types in an *acoustic* media. Significantly faster than FDWVEQ, but slower than RAY2D synthetics.	Acoustic rather than elastic. Large computer time.
Finite Difference Elastic (Program FDWVEQ)	2-D models, *exact* solution for *all* wave types in *elastic* media. Can be modified to include *Q*.	Extensive computer time and storage.

Table 4. Characteristics of methods of generating synthetic seismograms.

Method	*Characteristics*
Geometric ray theory	Analytic. Usefulness in tracing propagation path of wave energy depends on complexity of structure. Invalid when change in seismic velocity or curvature of wave front is large over a wavelength. Does not predict frequency-dependent effects.
Generalized ray theory (Cagniard-de Hoop)	Analytic. Spherical waves incident on planar interfaces. Incorporates specified direct, reflected, critically refracted, and Rayleigh waves. Integration in complex ray parameter plane and a Laplace transform. Validity of synthetic seismograms dependent on which rays are incorporated in solution. Truncation error results when finite number of rays is used.
Asymptotic ray theory	Analytic. Full solution is sum of infinite series of frequency-dependent terms. Asymptotic approximation, valid at high frequencies, consists of 1 or 2 terms. Additional terms necessary in the case of diffraction phenomena, curved interfaces, or inhomogeneous media. Increased accuracy of body-wave amplitudes obtained with various modifications of method.
Reflectivity	Analytic. Spherical waves propagating in plane-layered medium. Reflectivity term is costly to compute but need be computed only once for a given model. All internal multiples and conversions automatically included in reflectivity term. Two integrations required. Integration over limited range of real ray parameters restricts solution to body waves and introduces truncation error.
Full wave theory	Analytic. Real earth models (radial inhomogeneity) and smoothly varying velocity and density. Can incorporate ray paths involving turning points, near-grazing incidence, and critical incidence; multipathing; diffraction phenomena; and caustics. Uses frequency-dependent reflection and transmission coefficients. Two integrations required. Rays to be incorporated in solution must be specified.
Surface wave seismology	Analytic. Highly sensitive to structure of layered medium. Results usefully presented as dispersion curves. Body waves ignored. Representation in terms of multiply reflected, interfering plane waves valid only if distance from layer interface to source is large relative to layer thickness. Valid at

Table 4 (cont'd). Characteristics of methods of generating synthetic seismograms.

Method	*Characteristics*
Surface wave seismology (cont'd)	frequencies that are too low to meet high frequency approximation of ray/wave theory yet are high enough that required number of normal modes is prohibitive.
Normal modes	Analytic. Plane-layered waveguide handled readily. Valid at all frequencies but practical at low frequencies (smaller number of modes and so lower cost). Computational time reduced by employing Fast Field Program which can incorporate both normal and leaky modes. Costly, perhaps inefficient, in case of complex structure because normal modes must be recomputed whenever inhomogeneity in model is encountered.
Finite differences	Numerical. Displacement at grid points. Useful in near-field or with complex structure. Body waves or surface waves. Size of grid spacing affects stability and accuracy of results. Truncation error due to approximation to wave equation. Aliasing, numeric dispersion, and spurious reflected waves from artificial boundaries are potential problems. Costly due to number of computations and storage requirements.
Finite elements	Numerical. Displacements between grid points known by interpolation. Useful with irregularly shaped structure. Body waves or surface waves. Accuracy dependent on number of elements and method of interpolation. Aliasing, numeric dispersion, and spurious reflected waves from artificial boundaries are potential problems. Costly due to number of computations and storage requirements.

By presenting the characteristic features of each method, this report may overemphasize differences and unintentionally obscure similarities among the methods. It should be realized that the accuracy of synthetic seismograms generated by any of these methods is highly frequency dependent. Frequency (f) and equivalently wavelength ($\lambda = V/f$) serve as scale factors for a problem. The validity of the synthetic seismogram obtained is constrained by grid spacing relative to wavelength with numerical methods and by layer thickness relative to wavelength or change in velocity gradient over a wavelength in analytic approaches to solving the wave equation. The condition for the valid use of asymptotic approximations to replace exact quantities in the analytic solutions is generally $kr = 2\pi r/\lambda >> 1$, where r is the range from the source. In the far field, r is sufficiently large (at least 10 λ) that the condition is satisfied. The actual propagation distance required for far-field conditions to prevail is inversely proportional to frequency.

An understanding of the limitations and approximations inherent to the methods of generating synthetic seismograms, together with the selection of a method appropriate to a particular problem, is necessary if synthetic seismograms are to be used wisely and advantageously.

LITERATURE CITED

Aki, K. and P.G. Richards (1980) *Quantitative Seismology: Theory and Methods,* vol. I, II, San Francisco: W.H. Freeman and Company, 932 pp.

Alford, R.M., K.R. Kelly and D.M. Boore (1974) Accuracy of finite-difference modeling of the acoustic wave equation. *Geophysics,* **39**: 834–842.

Alterman, Z.S. and F.C. Karal, Jr. (1968) Propagation of elastic waves in layered media by finite difference methods. *Bulletin of the Seismological Society of America,* **58**: 367–398.

Alterman, Z.S. and D. Loewenthal (1972) Computer generated seismograms. In *Seismology: Body Waves and Sources* (B.A. Bolt, Ed.) *Methods in Computational Physics,* vol. 12, New York: Academic Press, pp. 35–164.

Alterman, Z.S. and A. Rotenberg (1969) Seismic waves in a quarter plane, *Bulletin of the Seismological Society of America*, **59**: 347-368.

Bolt, B.A. and W.D. Smith (1976) Finite-element computation of seismic anomalies for bodies of arbitrary shape. *Geophysics*, **41**: 145-150.

Boore, D.M. (1970) Love waves in nonuniform wave guides: Finite difference calculations. *Journal of Geophysical Research*, **75**: 1512-1527.

Boore, D.M. (1972) Finite difference methods for seismic wave propagation in heterogeneous materials. In *Seismology: Surface Waves and Earth Oscillations* (B.A. Bolt, Ed.), *Methods in Computational Physics*, vol. 11, New York: Academic Press, pp. 1-37.

Boore, D.M., K.L. Larner and K. Aki (1971) Comparison of two independent methods for the solution of wave-scattering problems: Response of a sedimentary basin to vertically incident *SH* waves. *Journal of Geophysical Research*, **76**: 558-569.

Braile, L.W., Chao Sheng Chiang and C.R. Daudt (1983) Synthetic seismogram calculations for two-dimensional velocity models. Final Technical Report no. ONR-1-83. Purdue University.

Brekhovskikh, L.M. (1960) *Waves in Layered Media.* Translated by D. Lieberman, New York: Academic Press, 561 pp.

Brekhovskikh, L.M. (1980) *Waves in Layered Media.* 2nd ed. Translated by D. Lieberman, New York: Academic Press, 503 pp.

Burdick, L.J. and J.A. Orcutt (1979) A comparison of the generalized ray and reflectivity methods of waveform synthesis. *Geophysical Journal of the Royal Astronomical Society*, **58**: 261-278.

Chander, R. (1977) On tracing seismic rays with specified end points in layers of constant velocity and plane interfaces. *Geophysical Prospecting*, **25**: 120-124.

Chapman, C.H. (1978) A new method for computing synthetic seismograms. *Geophysical Journal of the Royal Astronomical Society*, **54**: 481-518.

Choy, G.L., V.F. Cormier, R. Kind, G. Müller and P.G. Richards (1980) A comparison of synthetic seismograms of core phases generated by the full wave theory and by the reflectivity method. *Geophysical Journal of the Royal Astronomical Society*, **61**: 21-39.

Clay, C.S. and H. Medwin (1977) *Acoustical Oceanography: Principles and Applications,* New York: Wiley, 544 pp.

Clough, R.W. (1965) The finite element method in structural mechanics. In *Stress Analysis* (O.C. Zienkiewicz and G.S. Holister, Ed.), New York: Wiley, pp. 85-119.

Cooper, H.F. Jr. (1971) On the application of finite difference methods to study wave propagation in geologic materials. Air Force Weapons Laboratory, Technical Report AFWL-TR-70-171, 72 pp.

Coppens, A.B. (1982) An introduction to the parabolic equation for acoustic propagation. Naval Postgraduate School Technical Report NPS61-83-002, 44 pp.

Day-Sarkar, S.K. and C.H. Chapman (1978) A simple method for the computation of body-wave seismograms. *Bulletin of the Seismological Society of America*, **68**: 1577-1593.

Emerman, S.H., W. Schmidt and R.A. Stephen (1982) An implicit finite-difference formulation of the elastic wave equation. *Geophysics*, **47**: 1521-1526.

Ewing, W.M., W.S. Jardetzky and F. Press (1957) *Elastic Waves in Layered Media.* New York: McGraw-Hill, 380 pp.

Felsen, L.B. (1981) Hybrid ray-mode fields in inhomogeneous waveguides and ducts. *Journal of the Acoustical Society of America*, **69**: 352-361.

Felsen, L.B. and T. Ishihara (1979) Hybrid ray-mode formulation of ducted propagation. *Journal of the Acoustical Society of America*, **65**: 595-607.

Fertig, J. and G. Müller (1978) Computations of synthetic seismograms for coal seams with the reflectivity method. *Geophysical Prospecting*, **26**: 868-883.

Fuchs, K. (1968) The reflection of spherical waves from transition zones with arbitrary depth-dependent elastic moduli and density. *Journal of Physics of the Earth*, **16**: 27-41.

Fuchs, K. and G. Müller (1971) Computation of synthetic seismograms with the reflectivity method and comparison with observation. *Geophysical Journal of the Royal Astronomical Society*, **23**: 417–433.

Fuyuki, M. and Y. Matsumoto (1980) Finite difference analysis of Rayleigh wave scattering at a trench. *Bulletin of the Seismological Society of America*, **70**: 2051-2069.

Geller, R.J., G.A. Frazier and M.W. McCann, Jr. (1979) Dynamic finite element modeling of dislocations in a laterally heterogeneous crust. *Journal of Physics of the Earth*, **27**: 395–407.

Grant, F.S. and G.F. West (1965) *Interpretation Theory in Applied Geophysics.* New York: McGraw-Hill, 583 pp.

Greenhalgh, S.A. and D.W. King (1981) Curved raypath interpretation of seismic refraction data. *Geophysical Prospecting*, **29**: 853–882.

Halliday, D. and R. Resnick (1974) *Fundamentals of Physics.* New York: Wiley, 827 pp.

Herrmann, R.B. (1978) *Computer Programs in Earthquake Seismology, Vol. 2: Surface Wave Programs.* Saint Louis University Publication no. 241, Saint Louis, Missouri.

Hron, F. and E.R. Kanasewich (1971) Synthetic seismograms for deep seismic sounding studies using asymptotic ray theory. *Bulletin of the Seismological Society of America*, **61**: 1169–1200.

Hron, F., E.R. Kanasewich and T. Alpasian (1974). Partial ray expansion required to suitably approximate the exact wave solution. *Geophysical Journal of the Royal Astronomical Society*, **36**: 607–625.

Kamel, A. and L.B. Felsen (1981) Hybrid ray-mode formulation of SH motion in a two-layer half-space. *Bulletin of the Seismological Society of America*, **71**: 1763–1781.

Kelly, K.R. (1983) Numerical study of Love wave propagation. *Geophysics*, **48**: 833–853.

Kelly, K.R., R.W. Ward, S. Treitel and R.M. Alford (1976) Synthetic seismograms: A finite-difference approach. *Geophysics*, **41**: 2–27.

Kennett, B.L.N. (1979) Theoretical reflection seismograms for elastic media. *Geophysical Prospecting*, 27: 301–321.

Kennett, B.L.N. (1983) *Seismic Wave Propagation in Stratified Media.* New York: Cambridge University Press, 342 pp.

Kohketsu, K. (1981) Reinterpretation of seismograms obtained by the Kurayosi explosions with the reflectivity method. *Journal of Physics of the Earth*, **29**: 255–265.

Kolsky, H. (1953) *Stress Waves in Solids.* Oxford: Clarendon Press, 211 pp.

Krebes, E.S. and F. Hron (1981) Comparison of synthetic seismograms for anelastic media by asymptotic ray theory and the Thomson-Haskell method. *Bulletin of the Seismological Society of America*, **71**: 1463–1468.

Kutschale, H.W. (1973) Rapid computation by wave theory of propagation loss in the Arctic Ocean. Lamont-Doherty Geological Observatory Technical Report CU-8-73, 99 pp.

Lapidus, L. and G.F. Pinder (1982) *Numerical Solution of Partial Differential Equations in Science and Engineering.* New York: Wiley, 677 pp.

Lysmer, J. and L.A. Drake (1972) A finite element method for seismology. In *Seismology: Surface Waves and Earth Oscillations* (B.A. Bolt, Ed.), *Methods in Computational Physics*, vol. 11, New York: Academic Press, pp. 191–211.

McCowan, D.W., P. Glover and S.S. Alexander (1977) A static and dynamic finite element analysis of the 1971 San Fernando, California, earthquake. *Geophysical Journal of the Royal Astronomical Society*, **48**: 163–185.

McMechan, G.A. and W.D. Mooney (1980) Asymptotic ray theory and synthetic seismograms for laterally varying structures: Theory and application to the Imperial Valley, California. *Bulletin of the Seismological Society of America*, **70**: 2021–2035.

Melosh, H.J. and A. Raefsky (1981) A simple and efficient method for introducing faults into finite element computations. *Bulletin of the Seismological Society of America*, **71**: 1391–1400.

Müller, G. (1970) Exact ray theory and its application to the reflection of elastic waves from vertically inhomogeneous media. *Geophysical Journal of the Royal Astronomical Society*, **21**: 261-283.

Officer, C.B. (1974) *Introduction to Theoretical Geophysics.* New York: Springer-Verlag, 385 pp.

Pilant, W.L. (1979) *Elastic Waves in the Earth.* New York: Elsevier, 493 pp.

Press, F. and M. Ewing (1950) *Propagation of Elastic Waves in a Floating Ice Sheet.* Lamont Geological Observatory Technical Report 8.

Richtmyer, R.D. and K.W. Morton (1967) *Difference Methods for Initial-Value Problems,* 2nd ed. New York: Interscience, 399 pp.

Sato, R. and N. Hirata (1980) One method to compute theoretical seismograms in a layered medium. *Journal of Physics of the Earth*, **23**: 145-168.

Shtivelman, V. (1984) A hybrid method for wave field computation. *Geophysical Prospecting*, **32**: 236-257.

Smith, W.D. (1974) A nonreflecting plane boundary for wave propagation problems. *Journal of Computational Physics*, **15**: 492-503.

Smith, W.D. (1975) The application of finite element analysis to body wave propagation problems. *Geophysical Journal of the Royal Astronomical Society*, **42**: 747-768.

Takeuchi, H. and M. Saito (1972) Seismic surface waves. In *Methods in Computational Physics, Vol. 11, Seismology: Surface Waves and Earth Oscillations* (B.Bolt, Ed.), Academic Press, pp. 217-295.

Telford, W.M., L.P. Geldart, R.E. Sheriff and D.A. Keys (1976) *Applied Geophysics.* New York: Cambridge University Press, 860 pp.

Urick, R.J. (1979) *Sound Propagation in the Sea.* DARPA Report.

Urick, R.J. (1983) *Principles of Underwater Sound.* 3rd ed. New York: McGraw-Hill, 423 pp.

Wiggins, R.A. (1976) Body wave amplitude calculations II. *Geophysical Journal of the Royal Astronomical Society*, **46**: 1-10.

Wiggins, R.A. and J.A. Madrid (1974) Body wave amplitude calculations. *Geophysical Journal of The Royal Astronomical Society*, **37**: 423-433.

A facsimile catalog card in Library of Congress MARC format is reproduced below.

Peck, Lindamae
Review of methods for generating synthetic seismograms / by Lindamae Peck. Hanover, N.H.: U.S. Army Cold Regions Research and Engineering Laboratory; Springfield, Va.: available from National Technical Information Service, 1985.
v, 48 p., illus.; 28 cm. (CRREL Report 85-10.)
Prepared for Office of the Chief of Engineers by Corps of Engineers, U.S. Army Cold Regions Research and Engineering Laboratory under DA Project 4A161102-AT24.
Bibliography: p. 36.
1. Geophysics. 2. Ground motion. 3. Mathematical analysis. 4. Seismic signatures. 5. Seismology. 6. Synthetic seismograms. I. United States. Army. Corps of Engineers. II. Cold Regions Research and Engineering Laboratory, Hanover, N.H. V. Series: CRREL Report 85-10.

END

FILMED

10-85

DTIC